Non-Photochemical Laser-Induced Nucleation of Sulfathiazole in a Water/Ethanol Mixture

Wenjing Li, Aziza Ikni, Philippe Scouflaire, Xiaoxuan Shi, Nouha El Hassan, Pascale Gemeiner, Jean-Michel Gillet, Anne Spasojevic de Biré

Non-Photochemical Laser-Induced Nucleation of sulfathiazole in water/ethanol mixture

Li Wenjing[1,2], Aziza Ikni[1,2#], Philippe Scouflaire[1,3], Shi Xiaoxuan[1,2], Nouha El Hassan[1,2], Pascale Gemeiner[1,2], Jean-Michel Gillet[1,2], Anne Spasojević-de Biré[1,2]*

[1] Université Paris Saclay, CentraleSupélec, Campus de Châtenay, Grande Voie des Vignes, 92295 Châtenay-Malabry, France

[2] CNRS, UMR 8580, Laboratory "Structures Propriétés et Modélisation des Solides" (SPMS), Grande Voie des Vignes, 92295 Châtenay-Malabry, France

[3]CNRS, UPR 288, Laboratory "Energétique Moléculaire et Macroscopique, Combustion" (EM2C), Grande Voie des Vignes, 92295 Châtenay-Malabry, France

* Corresponding author

actual address: CINaM-CNRS, UMR 7325, Aix-Marseille Université, Campus de Luminy, F-13288 Marseille, France.

To be published in Crystal Growth and Design, manuscript ID cg-2015-01526z

Abstract

Non-Photochemical Laser-Induced Nucleation (NPLIN) is an original and promising nucleation method, which has been applied with success to small-molecule organic compounds, proteins and inorganic compounds, leading to almost 50 publications. After first application of NPLIN to glycine and carbamazepine, our team has performed NPLIN experiments on sulfathiazole (STZ) for the following reasons: i) STZ is considered as a model drug for studying polymorphism; ii) some STZ polymorphs present a two-dimensional (2D) packing type while others are with one-dimensional (1D) packing; iii) STZ solubility curves, crystal habits, crystallization characterization are well documented.

Firstly, we have determined the metastable zone limit of STZ in water/ethanol ($^{v}/_{v}$ 1:1) for three temperatures (15 °C, 25 °C and 40 °C). STZ metastable solutions have been irradiated with a non-focused nanosecond laser (532 nm) at 25 °C. Nucleation induction time and crystal habits have been compared with those obtained by spontaneous nucleation. Nucleation site is the air / solution interface. We have noted $Ind_{50}(\beta)$ the laser intensity required to induce nucleation with fifty percent efficiency for a given supersaturation coefficient β. The use of this index has allowed us to compare NPLIN experiments for different compounds in different solutions. A dependency of STZ crystal size and crystal number on the irradiation duration, i.e. pulse number, has been established. Moreover, the obtained crystals have been characterized by Raman spectroscopy and X-ray single crystal diffraction. The role of laser polarization (linear or circular) has been established in comparison with spontaneous nucleation. In order to gain a deeper understanding of this behavior, we have calculated *ab initio* interaction energies for all dimers existing in the different STZ polymorphs. Theoretical results are coherent with observation.

Short synopsis

Nucleation induction time and crystal habits of sulfathiazole (STZ) crystallized by Non-Photochemical Laser-Induced Nucleation (NPLIN) have been compared with those obtained by spontaneous nucleation. A dependency of STZ crystal size and crystal number on the irradiation duration, i.e., pulse number, has been established. The role of the laser polarization (linear or circular) has been demonstrated in comparison with spontaneous nucleation. In order to gain a deeper understanding of this behavior, we have calculated the *ab initio* interaction energies for all dimers existing in the different STZ polymorphs. The theoretical results are coherent with observation.

Key-words

Laser-Induced Nucleation, NPLIN, sulfathiazole, crystallization, polymorphism, interaction energy calculation

1. Introduction

Crystallization is a physicochemical process. It presents high theoretical complexity as well as considerable economic interest, mainly in the pharmaceutical industry, where 80 % of the dosage is in solid form.[1] Crystallization is essentially a separation and purification operation of organic and mineral products. It leads to the formation of a structured and organized solid through a state change from gas or liquid phase, as well as from a supersaturated solution in which the compound is dissolved. This paper focuses on crystallization of pharmaceutical products in solution. The solution is composed of a solvent and a solute. Nucleation and subsequent crystallization imply that a disequilibrium exists in solution. Nucleation could be generated in a variety of ways, depending on the solubility curve of the solute in the solvent. It could be generated by means of classical methods (solvent evaporation, temperature change, non-solvent addition or chemical reactions) or *via* more recent approaches (electric field application, ultrasonic waves, laser irradiation).

The term crystalline polymorphism[2] is used to qualify the relation between crystals of a same substance, which, generated *via* crystallization, give different crystalline structures. Crystalline polymorphism impacts the development of the crystalline product. The active ingredient polymorphism has significant effects on physical and chemical properties of the drug such as: density, hardness and fusion point, solubility, dissolution rate, bioavailability, mechanical properties and manufacturing process. Thus it requires careful control. Generally, only one crystallographic form displays the physicochemical properties which complies with the requisites of the expected final drug product. Particular efforts should be made to understand the physicochemical mechanisms which lead to the crystallization of one polymorph or another, in order to be able to design, and control its elaboration process. The mechanism mastering includes knowledge of physicochemical phenomena in crystallization

process. Classical methods generally focus on four parameters (temperature, supersaturation, crystallization media and hydrodynamic) influencing thermodynamic or kinetic of nucleation. Moreover, in the pharmaceutical context, the active polymorph is not always the thermodynamically most stable phase. The new approaches cited above allow in some cases a spatial or temporal or spatial-temporal nucleation control. Twenty years ago, Garetz *et al* [3] accidentally discovered a possible method to control nucleation. The authors have shown the possibility to induce the crystallization of urea from its supersaturated solution by a laser of 1064 nm. Afterwards, the Garetz's team further demonstrated the possibility to control the obtained polymorph *via* laser polarization on glycine[4] and L - (+) – histidine.[5] The authors called this method NPLIN for Non-Photochemical Laser-Induced Nucleation. We have recently extended[6] this acronym to all experiments where a nucleation was established *via* the use of laser and without photochemical reaction observed, (Scheme 1) even though some authors have not explicitly mentioned in their article a NPLIN method. In other words, if a solution (or a liquid) of a given solute (respectively a molecule) is exposed to a laser beam (whatever the laser type is) and the observed result is the crystallization of the solute, we will consider this experiment as NPLIN. Additionally, the putative mechanism, which has induced the nucleation, is not taken into account in our definition. The experiments, where crystals of the final product already exist in the solution, have been excluded from our definition. According to this definition, the literature[3-54] has considerably increased in the last five years (Figure S1). On the one hand, the observation of laser-induced nucleation is repeatable for various types of compounds, and on the other hand it seems possible to control crystallization by manipulating laser parameters. Some remarks should be made: i) nucleation induction time is dramatically reduced with NPLIN compared to spontaneous nucleation for solutions prepared under the same conditions; ii) crystal polymorph induced by laser shows a dependency on laser polarization for some small-molecule organic compounds like glycine,[4,

[8, 40], L-histidine[5] and carbamazepine;[47] iii) NPLIN has been applied to small-molecular organic compounds,[3-9, 11-14, 18, 27, 29, 31, 36-37, 39-42, 44-45, 47, 49-51, 54] proteins[10, 15-17, 19-20, 25-26, 28, 30, 32, 43, 48] as well as inorganic species[21-22, 24, 33-35, 38, 46] or some specific species;[23, 52] iv) nucleation can be induced with a single pulse,[42] a train of pulses or continuous wave (CW). One hypothesis[54] is that a linearly polarized laser interacts with clusters the polarisability tensor of which exhibits rod-like symmetry, while a circularly polarized laser interacts with clusters for which the polarizability tensor symmetry is disk-like. This possible mechanism is referred to as optical Kerr[8] effect hypothesis. By means of *ab initio* calculations of interaction energy for carbamazepine, we have demonstrated[47] that its polymorph, which presents a structure described as 1D packing, reacts preferentially with linearly polarized laser. On the contrary, the polymorph with 2D packing nucleates preferentially with circularly polarized laser. Our team has developed an automated NPLIN experimental set-up with multi-sample holder,[6] making it possible to realize a sufficient number of trials under the same conditions.

To experimentally further demonstrate the feasibility of NPLIN technique applied to drug molecules, a set of experiments with sulfathiazole (STZ) ($C_9H_9N_3O_2S_2$) (Scheme 2) dissolved in water/ethanol ($^{v}/_{v}$ 1:1) were undertaken. This drug has been used for more than 75 years and it is nowadays employed as an antibacterial for veterinary medication.[55-57] It is highly polymorphic and is often considered as a model compound for the study of polymorphism. Since its discovery in 1939,[58-59] numerous works have been done on isolation, production and characterization of its different polymorphic forms. The number of polymorphs has grown from two in 1941[60] to five in 1999.[61-62] STZ also exists as an amorphous compound,[63-64] hydrate[65] and more than hundred solvates.[66] There are currently 24 STZ crystal structures available in the Cambridge Structure Database (CSD) describing five different polymorphs, named FI, FII, FIII, FIV and FV. Charge density studies have been performed on STZ by Sovago *et al.* [67] and Shi *et al.* [68] Based on the work of Munroe *et al*,[69] between 10 °C and 50

°C, the stability order of the five polymorphs of STZ between 10 °C and 50 °C is proposed to be FI<FV<FIV<FII<FIII. According to these authors, FI is therefore less stable than FV in this temperature range. Various methods have been used to crystallize the different polymorphs and are reviewed by Abu Bakar.[70] As mentioned previously, laser polarization impact on the obtained crystal polymorph was initially explained by Garetz[8] as an optical Kerr effect. Within this context, STZ with its five polymorphs is a well suitable compound for NPLIN nucleation.

In this paper, we present a complete STZ NPLIN study. After the determination of the metastable zone limit (MZL) of STZ in water/ethanol ($^{v}/_{v}$ 1:1) mixture, STZ spontaneous nucleation by slow evaporation will be described. A large number of NPLIN experiments performed on adequate statistics will be reported in order to study the impact of different laser parameters. Finally, *ab initio* calculations of interaction energy will help to interpret how the laser polarization state affects the obtained crystal polymorphs.

2. Materials, methods and experiments

2.1 *Material*.

Commercial STZ (99%, white powder) was purchased from Alfa Aesar Company, and characterized as polymorph IV with both XRPD and Raman identification. The n-propanol and ethanol were obtained from VWR. Distilled water was made by internal distilled water generator. The absorption spectrum is given in Supplementary Material (Figure S2).

2.2 *Experimental laser irradiation set-up.*

An overview of the home-made set-up that we specially developed for the NPLIN experiments is given in Figure 1 and Figure S3. An annular laser light beam is generated by a Quanta-ray® Q-switched Nd:YAG laser, producing a 10 pulses per second train of linearly-polarized 7-ns laser pulses at 532 nm. The irradiation duration time control is achieved using

a shutter Thor Lab® (SC05 / SH 10). Reduction of the laser beam diameter has been been obtained through two types of equipments: a laboratory made telescope with a Nitrogen gas circulation for avoiding plasma discharge at the focal point and a commercial condenser (HEBX-3X from Melles Griot®). These equipments permit to reduce the beam diameter from 7 to 3.5 mm. Linearly polarized light is converted to circularly polarized one by sending it through a Glan polarizer followed by a Quarter Wave plate. A mirror is employed to reflect the beam by 90° in order to guide it towards the HPLC tube. In order to measure the exact laser intensity, a homemade glass plate is placed just after the shutter to collect 3 % of the coming beam; a wattmeter (QE25LB-S-MB) is used to monitor the beam power continuously. Solutions were contained in glass HPLC tubes. Each tube has a flat glass window mounted in the cap. Solutions were irradiated from above, with the laser beam entering the tube through the glass window in the cap, then entering the solution through the air/solution interface, and finally exiting through the bottom of the tube. More details on the experimental set-up can be found in the work of Clair *et al*.[6] The main advantages could be summarized as; i) 90 sample holders, allowing a sufficient redundancy; ii) a stable thermal bath; iii) a Yag-Nd laser at 532 nm; iv) a dedicated Labview® based software (irradiation time control, detailed record of input and output information, automated experiment); v) an *in situ* crystal growth monitored through a CCD camera connected to an inverted microscope. Table 1 summarizes the experimental conditions for the different experiments presented below.

2.3 *Solubility curve and STZ metastable zone determination.*

Solubility curves of STZ in different solvents have already been published.[70-72] Based on the work of Munroe *et al*,[71] we decided to use a mixture of water/ethanol ($^{v}/_{v}$ 1:1) for NPLIN experiment, due to the fact that STZ solubility is high in ethanol and the use of water/ethanol mixture allows a minimization of the evaporation during dissolution process. We have used STZ solubility in water/ethanol ($^{v}/_{v}$ 1:1) at 25 °C and 40 °C from Aaltonen's work,[73] and

measured the point at 15°C using the successive addition method described for carbamazepine by Detoisien *et al*.[74] The MZL of STZ in water/ethanol ($^{v}/_{v}$ 1:1) mixture is determined through the use of the same experimental set-up described by Ikni *et al*.[47]

2.4 *Spontaneous nucleation.*

Solutions of STZ in water, ethanol, water/ethanol ($^{v}/_{v}$ 1:1) and n-propanol with the same supersaturation coefficient (130%) were prepared and slowly evaporated for 120 hours. The supersaturation coefficient β is defined by C/C_s *100%, where C is the solution concentration (mg/ml) and C_s is the solubility at a given temperature.

2.5 *Supersaturated solution preparation and NPLIN experiments*.

Solutions were prepared according to the following procedure: i) solutions with supersaturation levels in the range of 110% to 170% were prepared in HPLC tubes (1 ml), which were adapted to fit our experimental needs;[6] ii) the solutions were heated to 55 °C in the carrousel until a complete dissolution of the STZ powder; iii) solutions were slowly cooled to the temperature of NPLIN experiments (25 °C) and then were aged from 18 hours to 24 hours before irradiation by laser light. The aging time permits formation of clusters in the solutions, thus to increase the probability of nucleation. Aging is a necessary prerequisite, which was confirmed by subsequent work on glycine[33-34, 36, 54] and L-histidine.[5] Depending on NPLIN experiments the solutions were exposed for a variable duration from 10 pulses (1s) to 600 pulses (60 s). The nucleation was followed by recording regularly micro photos at each tube bottom. After 3 hours, the tubes were opened, and then the crystals were filtered out and stored for characterization. Specific experimental conditions used in each experiment are reported in Table 1.

2.6 *STZ crystals characterization.*

STZ crystals were identified by single crystal X-Ray diffraction (Bruker D8 VENTURE), and by Raman spectroscopy (Dilor, excitation radiation was 632 nm). A first set of Raman spectra

have been collected after polymorph identification with the single X-ray diffraction. Raman spectra for each polymorph are acquired and used as reference for further polymorph identification (Figure S4). Due to the large number of crystals, Raman identification was made by sampling, and characterization of 15 to 20 crystals for each tube. The crystal habit was observed by *in situ* CCD camera and by the camera installed on the single crystal X-Ray diffractometer. Using a Matlab® image processing tool, we have been able to count the number of crystals in a given image.

2.7 *STZ theoretical calculations.*

Geometric parameters of polymorphs FII and FIII were extracted from the CSD (refcode SUTHAZ09, SUTHAZ11) while for polymorph FIV, we have used our experimental data.[68] The hydrogen atoms were put at their positions determined by thermal neutron diffraction for FII and FIII polymorphs. The interaction energy between a STZ molecule with each of its neighbour molecule for three polymorphs was computed in using Gaussian09 software.[75] The functional density theory (DFT) computation was carried out using the M06-2X functional and the cc-PVTZ basis set.

3. Results and discussion

3.1 STZ spontaneous nucleation in different solvents and metastable zone determination

As mentioned previously the mixture of water/ethanol ($^{v}/_{v}$1:1) was chosen *a priori* as a good solvent because the solubility of STZ is high in ethanol and the evaporation is limited by the use of water. Nevertheless spontaneous nucleation was tested also on pure solvents as reported in Table 2. In water/ethanol ($^{v}/_{v}$ 1:1) we obtained almost the same quantity of FIII and FIV; while FI occurred mostly in n-propanol; in ethanol, FII, FIII and FIV are equally distributed. Lastly water seemed to favor the crystallization of FIV. It should be noted that this work is the first report of NPLIN performed in a mixture of solvents.

STZ solubility curve in water/ethanol ($^{v}/_{v}$ 1:1) (Figure 2) was validated with the application of the Van't Hoff plot as shown in Figure S5 with R^2 = 0.988 as coefficient of determination. The equation is similar to that obtained by Abu Bakar *et al.*[70] The MZL was determined experimentally with the method described by Ikni *et al.*[47] As shown in Figure 2, no nucleation was observed in the STZ supersaturated solutions for 168 hours at three different temperatures even for the highest concentration. The critical super saturation β_c for STZ at 15 °C, 25 °C and 40 °C were estimated to be $\beta_{c,15}(168)$ = 180%; $\beta_{c,25}(168)$ = 170%; $\beta_{c,40}(168)$ = 170% respectively. A supersaturation coefficient at 25 °C corresponds to a concentration of 18.87 mg/ml of STZ. Therefore, for NPLIN experiments, all supersaturated solutions were prepared with a supersaturation coefficient lower than 170 % and the aging time of the solutions should be less than 168 hours. As a result, if crystallization from solution takes place under these conditions when exposed to laser irradiation, the latter can be considered as the cause of induced nucleation. In particular, for all NPLIN experiments in this work, new HPLC tubes were used in order to avoid heterogeneous or seeded nucleation.

3.2 STZ nucleation *via* NPLIN.

3.2.1 Reduction time of laser-induced nucleation and observation of nucleation site.

According to MZL measurement, a supersaturated solution of 170 % could remain metastable over more than one week. Figure 3 shows crystallization of STZ after receiving a 5 seconds laser irradiation. The first detectable STZ crystal (30 x 60 μm) appears after about 96 s (fourth image in Figure 3). Such observation has been repeated and the frequency is indicated in Table 1. According to Ikni *et al*,[47] one can define the induction time t_{in} as $t_{in} = t_{at} + t_{exp} + t_{NPLIN}$, where t_{at} corresponds to the necessary duration for the solution to reach and stay stable at NPLIN experimental temperature (25 °C in our case); $t_{at} \in [24, 48]$ h; t_{exp} corresponds to laser exposure duration; $t_{exp} = [1,60]$ s; t_{NPLIN} corresponds to the duration between the end of

the exposure and the observation of the crystal using the microscope; $t_{NPLIN} \in [0.026; 0.5]$ h. Therefore, according to the metastable zone ($\beta_{c,25}$(168 h) = 170%), observation of a shorter t_{in} indicates that laser light induces nucleation of STZ in water/ethanol ($^{v}/_{v}$ 1:1).

Moreover, we firstly observe a fuzzy crystal form, which seems falling down onto the bottom of the tube. A video of this behavior is available as supplementary material. The form appears fuzzy due to the fact the focal point corresponds to the bottom of the tubes. It indicates that crystals nucleate at the air-solution meniscus and sink when the weight suffices to overbalance the surface tension. A schematic representation of this behavior is given in Figure S6.

3.2.2 Crystal habit comparison in the case of spontaneous nucleation and in the case of laser induced nucleation.

The first photography of STZ crystals dated back to 1941 by Grove *et al.*[60] The authors reported hexagonal-like and rod-like crystals. Later on, Anwar *et al*[76] reviewed the crystal habits of FI, FII, FIII and FIV in different solvents. The consequences of crystal habit due to crystalization with additive,[77-78] or supercritical fluid crystalization,[78-80] the effect of temperature,[81-82] of solvent,[83-84] epitaxial growth[85] and grinding and moisture[86] have been extensively studied. An example of STZ crystal habits from spontaneous nucleation, LP NPLIN and CP NPLIN are given in Figure 4. One can easily remark that greater diversity of crystal habits and crystal size is observed in spontaneous nucleation, while NPLIN yields a more homogeneous distribution.

A set of single crystal X-Ray diffraction measurements has been carried out and FII, FIII and FIV were identified. The habits are given in Figure 5 associated with a variety of single crystal images. With a large number of crystals from NPLIN identified by single X-ray diffraction, we observed that crystal habits for all three polymorphs are quite diverse. FII

presents two major morphologies: square plates and hexagonal plates. FIII is usually observed as a prism, while FIV is frequently elongated or sometimes seen as a thin piece.

3.2.3 Impact of supersaturation coefficient and laser intensity on nucleation efficiency.

To study the effect of supersaturation coefficient β and laser intensity on nucleation efficiency, a number of NPLIN experiments were carried out to achieve reliable statistics; parameters values are given in Table 1. This means that for every experimental point, a number of tubes were prepared and processed under exactly the same conditions. The nucleation efficiency is obtained from the ratio of n (number of nucleated solutions induced by laser irradiation) to N (number of total irradiated solutions). The nucleation efficiency depends on the supersaturation coefficient β as well as on the laser intensity. Indeed, this is confirmed by the curves drawn in Figure 6 which give the nucleation fraction as a function of laser intensity for different supersaturation coefficient values and laser polarization.

In order to represent in one graph the correlation between supersaturation coeffecient and laser intensity, we have defined a new index Ind_{50} by mimetism of the inhibition biological index. We note $Ind_{50}(\beta)$ the laser intensity required to induce fifty percent nucleation for a given supersaturation coefficient β. The values of Ind_{50} for STZ in water/ethanol ($^{v}/_{v}$ 1:1), as function of supersaturation coefficient and laser polarization, are reported in Figure 7. It should be remarked that i) as previously observed in Figure 6, higher supersaturation tends to be associated with a lower laser intensity; ii) for identical laser intensity, LP is more efficient than CP. Results for carbamazepine (CBZ)[47] are also shown in Figure 7. Laser polarization shows opposite trends for CBZ (see last section). Six linear fits have been done over the 6 plots for the two compounds; regression coefficients are reported in Supplementary material (Figure S7, and Table S1). Although the experimental conditions (molecule, solvent, polarisation) are very different, regression curves are quite parallels. These lines allow a

prediction of optimum experimental parameters to achieve a nucleation efficiency of 50 %. As a matter of fact, our measurement with 170 % supersaturation has always given a nucleation efficiency higher than 50 %. The linearity assumption of the curve nucleation efficiency = f (intensity) for a given supersaturation is obviously not appropriate at low nucleation efficiency. In conclusion, this new index Ind_{50}, allows us to represent in one graph the behavior of two compounds in three different conditions, in other words, one can observe in one graph the results through six plots, instead of 19 curves.

3.2.4 Impact of laser irradiation time on nucleation efficiency and on induced crystal counting

Figure 8 shows the impact of laser irradiation time on crystal habits. It is clear that the longer the irradiation time is, the smaller and the more the crystals are. We have determined quantitatively how crystal average size and number were related to laser exposure time (Figure 9). It has to be noticed that the crystal number analysis corresponds to only 11 % of the irradiation beam surface, due to the fact that the camera does not cover the entire bottom of the tubes. Therefore, it is difficult to estimate the exact number of the obtained crystals. Nevertheless the variation tendency remains meaningful. Additionally, lower supersaturation is associated with smaller crystal number and smaller crystal size. The behavior observed in Figure 9 could be interpreted in the folowing way: i) the number of nucleation sites is a function of the irradiation time. For irradiation time of 1 s, *i.e.* number of pulses $\in$ [8, 12] if we take into account the uncertainty of the time to open the shutter, the ratio of crystal number to pulse number belongs to interval [1.1, 1.6] for LP, β = 130 %. This ratio increases to the interval [10, 15] for 30 s irradiation in the same conditions. For the most unfavorable conditions in term of efficiency (CP, β = 130 %) the ratio belongs to [1.1, 1.7] for 30 s irradiation. This number increases to interval [2.2, 3.4] for 60 s irradiation in the same

conditions. These observations indicate that with a supersatutration of 130 %, each LP pulse has induced about one crystal for 1s irradiation. Therefore, this provides an indicator to determine the limit of the irradiation time for a given set of conditions (polarisation, supersaturation, laser intensity). In other words, for a given polarisation, molecule and solvent, NPLIN is possible with a combination of supersaturation, laser intensity and irradiation time; for example, longer irradiation time will be required for NPLIN if laser intensity is decreased. ii) The impact of supersaturation on morphology behavior is easier to understand. Lower concentration implies a greater difficulty for the molecules to gather in a cluster to achieve a sufficient size to crystallize.

3.2.5 Impact of laser polarization on sulfathiazole polymorphism

Raman was used to identify the large number of STZ crystals. Crystals were carefully filtered (extracted from solution) shortly after irradiation: less than 3 hours. Characterization was carried out within the 2 following days to avoid polymorph transformation. With about 10 % to 20 % percent of crystals being identified, it turns out that most tubes contain a mixure of the three polymorphs (FII, FIII and FIV), but the proportion varies depending on the polarization type (LP or CP). This proportion differs from those observed for spontaneous nucleation. Polymorph distribution is shown in Figure 10. The number of each polymorph has been determined through a summation of the 15 to 20 crystals analyzed for each tube. It should be remarked that with spontaneous nucleation, equal quantity of FIII and FIV are obtained; with the method NPLIN, we modified the proportion of these two polymorphs, while the percentage of FII was unchanged. One can conclude that linear polarization favors FIV formation while circular polarization favors FIII. An explanation will be given in the next section.

3.2.6 Theoretical interaction energy determination and interpretation of polymorphism distribution

It has been demonstrated in the litterature for glycine,[4, 8, 40] L-histidine[5] and carbamazepine,[47] that laser polarization has an impact on crystal polymorphism. As described previously,[54] polarisability tensor symmetry of the clusters existing in the solution would explain the polarization effect on polymorphism. With the aim to increase our understanding of correlation between laser polarization and polymorphism, a methodology similar to those presented by Ikni *et al*[47] for carbamazepine polymorphism was followed. In this approach, we make the hypothesis that the interactions between the molecules in solution are of the same types than those observed in the crystal state (Figure 11). By calculating the different interaction energy of dimers existing with one molecule and each of its neighbouring molecule in each polymorph (Figure 11, step 1), we are able to estimate, which would be the preferential interactions in the solution state. Then, we rank the interaction energies by decreasing values (Figure 11, step 2) and determine the symmetry (dimer, 1D, 2D or 3D) of the objects (Figure 11, step 3) formed by taking into account the first (or the first two) interactions. Finaly, a threshold in terms of energy is used to discriminate (if possible) between the different polymorphs (Figure 11, step 4). This method has been succesfully used for carbamazepine. Carbamazepine form I appears to be more "1D" than carbamazepine form III, in agreement with the fact that NPLIN has yielded more carbamazepine form I with LP than with CP in acetonitrile. For polymorph FII, FIII and FIV of STZ, we have calculated interaction energy for all dimers formed by a molecule and each of its neighbouring molecules taken two by two. The results are summarized in the Figure 12 and Table S2. *Ab initio* quantum computation calculation by Gaussian09, [75] provided an estimate of interaction energy of different dimers for the three polymorphs of STZ, *i.e.* FII, FIII and FIV. FIII and FIV are the most stable forms at ambient temperature.[70] This is in agreement with this

calculation (-44.2048 kJ.mol^{-1} for FIV, -42.5482 kJ.mol^{-1} for FIII and -33.7494 kJ.mol^{-1} for FII). The packing formed by the interactions possessing an energy ⩾ 32 kJ.mol^{-1} gives a 3D packing type for FIII, and a 2D packing type for FII and FIV, while at a greater energy (⩾ 40 kJ.mol^{-1}) a 2D packing type for FIII, and a 1D packing type for FIV. The threshold chosen (⩾ 40 kJ.mol^{-1}) corresponds to a large domain (Figure 12). Therefore, it seems reasonnable that the main interactions in the solution state belong to those greater than this threshold. The packing type observed for the two forms (FIII, 2D), (FIV, 1D) for an energy interaction ⩾ 40 kJ.mol^{-1} could be correlated to the different polymorph distribution obtained with CP or LP. FIII dominates with CP, while FIV dominates with LP, according to the mechanism described as follows: a cluster with a polarisability tensor symmetry of 2D will interact with CP while a cluster with a polarisability tensor symmetry of 1D will interact with LP.[47]

Hence, in our opinion, the understanding of the mechanism behind the NPLIN could be understood in two aspects: the first one concerns the reason why NPLIN reduces nucleation induction time within the metastble zone; the second one concerns the impact of laser polarization. Our calculations support the explanation concerning the second aspect. The assumption is that clusters of the two symmetries exist in the solution (they are built with interactions of the same energy) and laser polarization favors the nucleation of the clusters of the same symmetry (1D with LP, 2D with CP).

Additionally, one can note (Figure 5) that FII was observed as hexagonal plaques; FIII was shown in form of prism; and FIV was elongated like a rod, eventhough the crystal habit (depending on the crystal growth, kinetics) could not be correlated to crystal packing mode.

4. Conclusion

This work demonstrates for the first time the experimental feasibility of NPLIN method on STZ. The MZL of STZ in water/ethanol ($^{v}/_{v}$ 1:1) is measured for three temperatures 15 °C, 25

°C and 40 °C. Spontaneous nucleation requires at least 168 hours, while NPLIN method can induce nucleation within 30 mins after irradiation for solutions aged for 24 hours. Crystal habits differ between spontaneous nucleation and NPLIN. Nucleation site is the air / solution interface. A dependency of crystal sizes and crystal counting with irradiation duration, *i.e.*, pulse number, is found. More precisely, with the increase of pulse number, the amount of crystals induced by NPLIN increases, while the average size of crystals decreases. Nucleation efficiency depends on the supersaturation and laser intensity. After characterization by Raman spectroscopy and by single crystal X-ray diffraction, differences in polymorph distribution is observed between spontaneous nucleation, NPLIN with LP and NPLIN with CP. Therefore, the role of laser polarization is established. NPLIN with LP yielded a majority of FIV, while FIII is the dominant product when NPLIN with CP is applied. *Ab initio* theoretical interaction energy calculations permit us to explore the hypothesis of polarization-dependency. Indeed, FIV of STZ tends to form molecular packing in 1D; and FIII of STZ tends to form a 2D packing. Therefore, a correlation is observed between cluster packing symmetry and laser polarization for NPLIN experiment. This is in agreement with the hypothesis proposed by Garetz *et al*.[8] Our calculations do not yet have the ambition to fully model the nucleation mechanism, but only to shed new light on the Kerr effect hypothesis concerning to the role of laser polarization on polymorphism. Our previous observations on carbamazepine[47] show similar trend. Such correlation is currently investigated for different small-molecule organic compounds.

Bubbling due to heating has been observed by several researchers[14, 18, 20, 26, 30, 33, 37] only when focused laser was used. Cavitation bubbles are observed to form and collapse within about 50 μs in case of supersaturated aqueous carbon dioxide solutions.[31] Indeed, the cavitation bubble behavior was monitored with a high-speed imaging camera. This is different from our experimental conditions (a non-focused laser beam, a detection after 4 s of the first pulse). In

our case, the solution is transparent and there is no absorption at the given wavelength (532 nm). Moreover, even if the exposed solution absorbed the entire pulse, the duration is so short (7ns) that the temperature rise would be less than 1 °C and consequently no bulk heating can be ruled out, while a strong heating at molecular level cannot be excluded.[87] Besides, no cavitation bubbles have been observed in our NPLIN experiments.

Acknowledgements

This work was supported by the ANR Pnano "NPLIN_4_drug".

Supplementary Material

14 pages. **Table S1.** Equations and R-factors of the linear regression of the Ind_{50} of Figure 7. **Table S2**. Theoretical interaction energy ($kJ.mol^{-1}$) for STZ polymorphs II, III and IV. **Figure S1**. NPLIN publications[3-54] growth (1996-2015) according to definition in Scheme 1. **Figure S2**. Absorption spectrum of a solution of STZ in water/ethanol ($^{v}/_{v}$ 1:1) realized with a Jasco spectrophotometer V630 bio. **Figure S3**. Experimental set-up, details. **Figure S4**. Raman spectra of the different polymorphs of STZ. **Figure S5.** Van't Hoff equation solubility fit (y=-5.88x+22.01, R^2=0.988). **Figure S6**. Schematic representation of the nucleation site. Step 1. The STZ molecules agglomerate in a cluster just after the irradiation. Step 2. The STZ nucleates and crystals grow. Step 3. The STZ crystal becomes bigger and falls to the bottom of the tube. Step 4. The STZ crystal is on the bottom of the tube where the camera is focalized. The crystal then continues to grow. The scheme is not at the scale. **Figure S7.** Representation of the coefficient of the linear fit of Figure 7. A vertical line indicates that the fit lines are parallel. **Video S1**. Experimental demonstration of NPLIN with STZ in water/ethanol ($^{v}/_{v}$ 1:1). T = 25°C, SS = 170 %, t_{irr} = 5 s, laser intensity = 0.23 $GW.cm^{-2}$, sample volume = 1 ml.

References

1. Leuenberger, H.; Leuenberger, M. N.; Puchkov, M., Implementing virtual R&D reality in industry: *In silico* design and testing of solid dosage forms. *Swiss Pharma* **2009,** *31*, 7-8.

2. Bernstein, J., *Polymorphism in molecular crystals*. Oxford University Press, 2007; Vol. 14.

3. Garetz, B. A.; Aber, J. E.; Goddard, N. L.; Young, R. G.; Myerson, A. S., Nonphotochemical, Polarization-Dependent, Laser-Induced Nucleation in Supersaturated Aqueous Urea Solutions. *Phys. Rev. Lett.* **1996,** *77*, 3475-3476.

4. Sun, X. Y.; Garetz, B. A.; Myerson, A. S., Supersaturation and polarization dependence off polymorph control in the nonphotochemical laser-induced nucleation (NPLIN) of aqueous glycine solutions. *Cryst. Growth Des.* **2006,** *6*, 684-689.

5. Sun, X.; Garetz, B. A.; Myerson, A. S., Polarization Switching of Crystal Structure in the Nonphotochemical Laser-Induced Nucleation of Supersaturated Aqueousl-Histidine. *Cryst. Growth Des.* **2008,** *8*, 1720-1722.

6. Clair, B.; Ikni, A.; Li, W.; Scouflaire, P.; Quemener, V.; Spasojević-de Biré, A., A new experimental setup for high-throughput controlled non-photochemical laser-induced nucleation: application to glycine crystallization. *J. Appl. Crystallogr.* **2014,** *47*, 1252-1260.

7. Zaccaro, J.; Matić, J.; Myerson, A. S.; Garetz, B. A., Nonphotochemical, Laser-Induced Nucleation of Supersaturated Aqueous Glycine Produces Unexpected γ-Polymorph. *Cryst. Growth Des.* **2001,** *1*, 5-8.

8. Garetz, B. A.; Matić, J.; Myerson, A. S., Polarization Switching of Crystal Structure in the Nonphotochemical Light-Induced Nucleation of Supersaturated Aqueous Glycine Solutions. *Phys. Rev. Lett.* **2002,** *89*.175501-1-4.

9. Tsunesada, F.; Iwai, T.; Watanabe, T.; Adachi, H.; Yoshimura, M.; Mori, Y.; Sasaki, T., High-quality crystal growth of organic nonlinear optical crystal DAST. *J. Cryst. Growth* **2002,** *237*, 2104-2106.

10. Adachi, H.; Takano, K.; Hosokawa, Y.; Inoue, T.; Mori, Y.; Matsumura, H.; Yoshimura, M.; Tsunaka, Y.; Morikawa, M.; Kanaya, S.; Masuhara, H.; Kai, Y.; Sasaki, T., Laser Irradiated Growth of Protein Crystal. *Jpn. J. Appl. Phys.* **2003,** *42*, L798-L800.

11. Hosokawa, Y.; Adachi, H.; Yoshimura, M.; Mori, Y.; Sasaki, T.; Masuhara, H., Femtosecond laser-induced crystallization of 4-(dimethylamino)-N-methyl-4-stilbazolium tosylate. *Cryst. Growth Des.* **2005,** *5*, 861-863.

12. Matić, J.; Sun, X. Y.; Garetz, B. A.; Myerson, A. S., Intensity, wavelength, and polarization dependence of nonphotochemical laser-induced nucleation in supersaturated aqueous urea solutions. *Cryst. Growth Des.* **2005,** *5*, 1565-1567.

13. Yoshikawa, H. Y.; Hosokawa, Y.; Masuhara, H., Spatial control of urea crystal growth by focused femtosecond laser irradiation. *Cryst. Growth Des.* **2006,** *6*, 302-305.

14 13bis = 86. Yoshikawa, H. Y.; Hosokawa, Y.; Masuhara, H., Explosive crystallization of urea triggered by focused femtosecond laser irradiation. *Jpn. J. Appl. Phys.* **2006,** *45*, L23-L26.

15. 14 Kashii, M.; Hosokawa, Y.; Kitano, H.; Adachi, H.; Mori, Y.; Takano, K.; Matsumura, H.; Inoue, T.; Murakami, S.; Sugamoto, K.; Yoshikawa, H.; Sasaki, T.; Masuhara, H., Femtosecond laser-induced cleaving of protein crystal in water solution. *Appl. Surf. Sci.* **2007,** *253*, 6447-6450.

16. 15 Nakamura, K.; Sora, Y.; Yoshikawa, H. Y.; Hosokawa, Y.; Murai, R.; Adachi, H.; Mori, Y.; Sasaki, T.; Masuhara, H., Femtosecond laser-induced crystallization of protein in gel medium. *Appl. Surf. Sci.* **2007,** *253*, 6425-6429.

17. 16. Tsuboi, Y.; Shoji, T.; Kitamura, N., Crystallization of lysozyme based on molecular assembling by photon pressure. *Jpn. J. Appl. Phys.* **2007,** *46*, L1234-L1236.

18. 16bis = 85. Nakamura, K.; Hosokawa, Y.; Masuhara, H., Anthracene crystallization induced by single-shot femtosecond laser irradiation: Experimental evidence for the important role of bubbles. *Cryst. Growth Des.* **2007,** *7*, 885-889.

19. 17. Lee, I. S.; Evans, J. M. B.; Erdemir, D.; Lee, A. Y.; Garetz, B. A.; Myerson, A. S., Nonphotochemical Laser Induced Nucleation of Hen Egg White Lysozyme Crystals. *Cryst. Growth Des.* **2008,** *8*, 4255-4261.

20. 17bis = 84. Yoshikawa, H. Y.; Murai, R.; Maki, S.; Kitatani, T.; Sugiyama, S.; Sazaki, G.; Adachi, H.; Inoue, T.; Matsumura, H.; Takano, K., Laser energy dependence on femtosecond laser-induced nucleation of protein. *Appl. Phys. A: Mater. Sci. Process.* **2008**, *93*, 911-915.

21. 18. Alexander, A. J.; Camp, P. J., Single Pulse, Single Crystal Laser-Induced Nucleation of Potassium Chloride. *Cryst. Growth Des.* **2009,** *9*, 958-963.

22. 19. Duffus, C.; Camp, P. J.; Alexander, A. J., Spatial control of crystal nucleation in agarose gel. *J. Am. Chem. Soc.* **2009,** *131*, 11676-11677.

23. 20. Sun, X.; Garetz, B. A.; Moreira, M. F.; Palffy-Muhoray, P., Nonphotochemical laser-induced nucleation of nematic phase and alignment of nematic director from a supercooled thermotropic liquid crystal. *Phys. Rev. E* **2009,** *79*, 021701-1-6.

24. 21. Ward, M. R.; Ballingall, I.; Costen, M. L.; McKendrick, K. G.; Alexander, A. J., Nanosecond pulse width dependence of nonphotochemical laser-induced nucleation of potassium chloride. *Chem. Phys. Lett.* **2009,** *481*, 25-28.

25. 22. Yoshikawa, H. Y.; Murai, R.; Sugiyama, S.; Sazaki, G.; Kitatani, T.; Takahashi, Y.; Adachi, H.; Matsumura, H.; Murakami, S.; Inoue, T.; Takano, K.; Mori, Y.,

Femtosecond laser-induced nucleation of protein in agarose gel. *J. Cryst. Growth* **2009,** *311*, 956-959.

26. 23. Murai, R.; Yoshikawa, H. Y.; Takahashi, Y.; Maruyama, M.; Sugiyama, S.; Sazaki, G.; Adachi, H.; Takano, K.; Matsumura, H.; Murakami, S.; Inoue, T.; Mori, Y., Enhancement of femtosecond laser-induced nucleation of protein in a gel solution. *Appl. Phys. Lett.* **2010,** *96*, 043702-1-3.

27. 24. Rungsimanon, T.; Yuyama, K.-i.; Sugiyama, T.; Masuhara, H., Crystallization in Unsaturated Glycine/D_2O Solution Achieved by Irradiating a Focused Continuous Wave Near Infrared Laser. *Cryst. Growth Des.* **2010,** *10*, 4686-4688.

28. 25. Yennawar, N.; Denev, S.; Gopalan, V.; Yennawar, H., Laser-improved protein crystallization screening. *Acta Crystallogr., Sect. F: Struct. Biol. Cryst. Commun.* **2010,** *66*, 969-972.

29. 26. Yuyama, K.; Sugiyama, T.; Masuhara, H., Millimeter-Scale Dense Liquid Droplet Formation and Crystallization in Glycine Solution Induced by Photon Pressure. *J. Phys. Chem. Lett.* **2010,** *1*, 1321-1325.

30. 27. Iefuji, N.; Murai, R.; Maruyama, M.; Takahashi, Y.; Sugiyama, S.; Adachi, H.; Matsumura, H.; Murakami, S.; Inoue, T.; Mori, Y.; Koga, Y.; Takano, K.; Kanaya, S., Laser-induced nucleation in protein crystallization: Local increase in protein concentration induced by femtosecond laser irradiation. *J. Cryst. Growth* **2011,** *318*, 741-744.

31. 28. Knott, B. C.; LaRue, J. L.; Wodtke, A. M.; Doherty, M. F.; Peters, B., Communication: Bubbles, crystals, and laser-induced nucleation. *J. Chem. Phys.* **2011,** *134*, 171102-1-4.

32. 29. Murai, R.; Yoshikawa, H. Y.; Hasenaka, H.; Takahashi, Y.; Maruyama, M.; Sugiyama, S.; Adachi, H.; Takano, K.; Matsumura, H.; Murakami, S.; Inoue, T.; Mori, Y.,

Influence of energy and wavelength on femtosecond laser-induced nucleation of protein. *Chem. Phys. Lett.* **2011,** *510*, 139-142.

33. 30. Soare, A.; Dijkink, R.; Pascual, M. R.; Sun, C.; Cains, P. W.; Lohse, D.; Stankiewicz, A. I.; Kramer, H. J. M., Crystal Nucleation by Laser-Induced Cavitation. *Cryst. Growth Des.* **2011,** *11*, 2311-2316.

34. 31. Ward, M. R.; Copeland, G. W.; Alexander, A. J., Chiral hide-and-seek: retention of enantiomorphism in laser-induced nucleation of molten sodium chlorate. *J. Chem. Phys.* **2011,** *135*, 114508-1-8.

35. 32. Jacob, J. A.; Sorgues, S.; Dazzi, A.; Mostafavi, M.; Belloni, J., Homogeneous Nucleation-Growth Dynamics Induced by Single Laser Pulse in Supersaturated Solutions. *Cryst. Growth Des.* **2012,** *12*, 5980-5985.

36. 33. Sugiyama, T.; Yuyama, K.; Masuhara, H., Laser trapping chemistry: from polymer assembly to amino acid crystallization. *Acc. Chem. Res.* **2012,** *45*, 1946-1954.

37. 34. Uwada, T.; Fujii, S.; Sugiyama, T.; Usman, A.; Miura, A.; Masuhara, H.; Kanaizuka, K.; Haga, M. A., Glycine crystallization in solution by CW laser-induced microbubble on gold thin film surface. *ACS Appl. Mater. Interfaces* **2012,** *4* (3), 1158-1163.

38. 35. Ward, M. R.; Alexander, A. J., Nonphotochemical Laser-Induced Nucleation of Potassium Halides: Effects of Wavelength and Temperature. *Cryst. Growth Des.* **2012,** *12*, 4554-4561.

39. 36. Ward, M. R.; McHugh, S.; Alexander, A. J., Non-photochemical laser-induced nucleation of supercooled glacial acetic acid. *Phys. Chem. Chem. Phys.* **2012,** *14*, 90-93.

40. 37. Yuyama, K.-I.; Rungsimanon, T.; Sugiyama, T.; Masuhara, H., Selective Fabrication of α- and γ-Polymorphs of Glycine by Intense Polarized Continuous Wave Laser Beams. *Cryst. Growth Des.* **2012,** *12*, 2427-2434.

41. 38. Yuyama, K.-i.; Rungsimanon, T.; Sugiyama, T.; Masuhara, H., Formation, Dissolution, and Transfer Dynamics of a Millimeter-Scale Thin Liquid Droplet in Glycine Solution by Laser Trapping. *J. Phys. Chem. C* **2012,** *116*, 6809-6816.

42. 39. Liu, T.-H.; Uwada, T.; Sugiyama, T.; Usman, A.; Hosokawa, Y.; Masuhara, H.; Chiang, T.-W.; Chen, C.-J., Single femtosecond laser pulse-single crystal formation of glycine at the solution surface. *J. Cryst. Growth* **2013,** *366*, 101-106.

43. 40. Nakayama, S.; Yoshikawa, H. Y.; Murai, R.; Kurata, M.; Maruyama, M.; Sugiyama, S.; Aoki, Y.; Takahashi, Y.; Yoshimura, M.; Nakabayashi, S.; Adachi, H.; Matsumura, H.; Inoue, T.; Takano, K.; Murakami, S.; Mori, Y., Effect of Gel–Solution Interface on Femtosecond Laser-Induced Nucleation of Protein. *Cryst. Growth Des.* **2013,** *13*, 1491-1496.

44. 41. Spasojević-de Biré, A., A change of phase. *International innovation* **2013**, 44-46.

45. 42. Belloni, J.; Spasojević-de Biré, A.; Sorgues, S.; Mostafavi, M.; Scouflaire, P.; Ghermani, N.-E., Cristallogenèse déclenchée par impulsion laser. *L'actualité chimique* **2014**, 77-84.

46. 43. Fang, K.; Arnold, S.; Garetz, B. A., Nonphotochemical Laser-Induced Nucleation in Levitated Supersaturated Aqueous Potassium Chloride Microdroplets. *Cryst. Growth Des.* **2014,** *14*, 2685-2688.

47. 44. Ikni, A.; Clair, B.; Scouflaire, P.; Veesler, S.; Gillet, J.-M.; El Hassan, N.; Dumas, F.; Spasojević-de Biré, A., Experimental Demonstration of the Carbamazepine Crystallization from Non-photochemical Laser-Induced Nucleation in Acetonitrile and Methanol. *Cryst. Growth Des.* **2014,** *14*, 3286-3299.

48 45. Yoshikawa, H. Y.; Murai, R.; Adachi, H.; Sugiyama, S.; Maruyama, M.; Takahashi, Y.; Takano, K.; Matsumura, H.; Inoue, T.; Murakami, S.; Masuhara, H.; Mori, Y.,

Laser ablation for protein crystal nucleation and seeding. *Chem. Soc. Rev.* **2014,** *43*, 2147-2158.

49 46. Yuyama, K.; Wu, C. S.; Sugiyama, T.; Masuhara, H., Laser trapping-induced crystallization of L-phenylalanine through its high-concentration domain formation. *Photochem. Photobiol. Sci.* **2014,** *13*, 254-260.

50 47. Bartkiewicz, S.; Miniewicz, A., Whirl-enhanced continuous wave laser trapping of particles. *Phys. Chem. Chem. Phys.* **2015,** *17*, 1077-1083.

51 48. Ikeda, K.; Maruyama, M.; Takahashi, Y.; Mori, Y.; Yoshikawa, H. Y.; Okada, S.; Adachi, H.; Sugiyama, S.; Takano, K.; Murakami, S.; Matsumura, H.; Inoue, T.; Yoshimura, M.; Mori, Y., Selective crystallization of the metastable phase of indomethacin at the interface of liquid/air bubble induced by femtosecond laser irradiation. *Appl. Phys. Express* **2015,** *8*, 045501-1-4.

52 49. Ward, M. R.; Jamieson, W. J.; Leckey, C. A.; Alexander, A. J., Laser-induced nucleation of carbon dioxide bubbles. *J. Chem. Phys.* **2015,** *142*, 144501-1-8.

53. 50. Ward, M. R.; Rae, A.; Alexander, A. J., Nonphotochemical Laser-Induced Crystal Nucleation by an Evanescent Wave. *Cryst. Growth Des.* **2015,** *15* (9), 4600-4605.

54. 51. Matić, J., Non-photochemical light-induced nucleation and control of polymorphism through polarization-switching. Ph.D. Dissertation, Polytechnic University, **2005**.

55. 52. Smith, D. A.; Barker, I. K.; Allen, O., The effect of certain topical medications on healing of cutaneous wounds in the common garter snake (Thamnophis sirtalis). *Can. J. Vet. Res. 1***988**, 52, 129-133.

56. 53. Budavari, S., *The Merck index: an encyclopedia of chemicals, drugs, and biologicals*. Merck: Whitehouse Station, NJ, **1996**.

57. 54. Kahn, C.M.; T *The Merck index: an encyclopedia of chemicals, drugs, and biologicals*. Merck: Whitehouse Station, NJ **2005**, pp 2076.

58. 55. Lott, W.; Bergeim, F. H., 2-(p-Aminobenzenesulfonamido)-thiazole: a new chemotherapeutic agent. *J. Am. Chem. Soc.* **1939,** *61*, 3593-3594.

59. 56. Fosbinder, R. J.; Walter, L., Sulfanilamido derivatives of heterocyclic amines. *J. Am. Chem. Soc.* **1939,** *61*, 2032-2033.

60. 57. Grove, D. C.; Keenan, G. L., The dimorphism of sulfathiazole. *J. Am. Chem. Soc.* **1941,** *63*, 97-99.

61. 58. Hughes, D. S.; Hursthouse, M. B.; Threlfall, T.; Tavener, S., A new polymorph of sulfathiazole. *Acta Crystallogr., Sect. C: Cryst. Struct. Commun.* **1999,** *55*, 1831-1833.

62. 59. Chan, F. C.; Anwar, J.; Cernik, R.; Barnes, P.; Wilson, R., *Ab initio* structure determination of sulfathiazole polymorph V from synchrotron X-ray powder diffraction data. *J. Appl. Crystallogr.* **1999,** *32*, 436-441.

63. 60. Lagas, M.; Lerk, C., The polymorphism of sulphathiazole. *Int. J. Pharm. (Amsterdam, Neth.)* **1981,** *8*, 11-24.

64. 61. Mesley, R.; Houghton, E., Infrared identification of pharmaceutically important sulphonamides with particular reference to the occurrence of polymorphism. *J. Pharm. Pharmacol.* **1967,** *19*, 295-304.

65. 62. Kuhnert-Brandstätter, M.; Wunsch, S., Polymorphie und Mischkristallbildung bei Sulfonamiden und verwandten Verbindungen. *Microchim. Acta* **1969,** *57*, 1297-1307.

66. 63. Bingham, A. L.; Hughes, D. S.; Hursthouse, M. B.; Lancaster, R. W.; Tavener, S.; Threlfall, T. L., Over one hundred solvates of sulfathiazole *Chem. Commun. (Cambridge, U. K.)* **2001**, 603-604.

67. 64. Sovago, I.; Gutmann, M. J.; Hill, J. G.; Senn, H. M.; Thomas, L. H.; Wilson, C. C.; Farrugia, L. J., Experimental Electron Density and Neutron Diffraction Studies on the Polymorphs of Sulfathiazole. *Cryst. Growth Des.* **2014,** *14*, 1227-1239.

68. 65. Shi, X.; El Hassan, N.; Ikni, A.; Bouhenache, S.; Li, W.; Guiblin, N; Spasojević-de Biré A. ;Ghermani, N-E., Charge Density Study of Piroxicam Tautomers. *CrystEngComm.*, **2016,** in revision,

69 66. Munroe, Á.; Rasmuson, Å. C.; Hodnett, B. K.; Croker, D. M., Relative Stabilities of the Five Polymorphs of Sulfathiazole. *Cryst. Growth Des* **2012,** *12*, 2825-2835.

70. 67. Abu Bakar, M. R.; Nagy, Z. K.; Rielly, C. D.; Dann, S. E., Investigation of the riddle of sulfathiazole polymorphism. *Int. J. Pharm. (Amsterdam, Neth.)* **2011,** *414*, 86-103.

71. 68. Munroe, A. i.; Rasmuson, Å. C.; Hodnett, B. K.; Croker, D. M., Relative stabilities of the five polymorphs of sulfathiazole. *Cryst. Growth Des.* **2012,** *12*, 2825-2835.

72. 69. Khoshkhoo, S.; Anwar, J., Crystallization of polymorphs: the effect of solvent. *J. Phys. D: Appl. Phys.* **1993,** *26*, B90-B93.

73. 70. Aaltonen, J. *P*olymorph screening of sulfathiazole, Master's Thesis, University of Helsinki, **2002**.

74. 71. Detoisien, T.; Forite, M.; Taulelle, P.; Teston, J.; Colson, D.; Klein, J. P.; Veesler, S., A rapid method for screening crystallization conditions and phases of an active pharmaceutical ingredient. *Org. Process Res. Dev.* **2009,** *13*, 1338-1342.

75. 72. Frisch, M. J.; Trucks, G. W.; Schlegel, H. B.; Scuseria, G. E.; Robb, M. A.; Cheeseman, J. R.; Scalmani, G.; Barone, V.; Mennucci, B.; Petersson, G. A.; Nakatsuji, H.; Caricato, M.; Li, X.; Hratchian, H. P.; Izmaylov, A. F.; Bloino, J.; Zheng, G.; Sonnenberg, J. L.; Hada, M.; Ehara, M.; Toyota, K.; Fukuda, R.; Hasegawa, J.; Ishida, M.; Nakajima, T.; Honda, Y.; Kitao, O.; Nakai, H.; Vreven, T.; Montgomery, J. A., Jr.; Peralta, J. E.; Ogliaro, F.; Bearpark, M.; Heyd, J. J.; Brothers, E.; Kudin, K. N.; Staroverov, V. N.; Kobayashi, R.;

Normand, J.; Raghavachari, K.; Rendell, A.; Burant, J. C.; Iyengar, S. S.; Tomasi, J.; Cossi, M.; Rega, N.; Millam, J. M.; Klene, M.; Knox, J. E.; Cross, J. B.; Bakken, V.; Adamo, C.; Jaramillo, J.; Gomperts, R.; Stratmann, R. E.; Yazyev, O.; Austin, A. J.; Cammi, R.; Pomelli, C.; Ochterski, J. W.; Martin, R. L.; Morokuma, K.; Zakrzewski, V. G.; Voth, G. A.; Salvador, P.; Dannenberg, J. J.; Dapprich, S.; Daniels, A. D.; Farkas, O.; Foresman, J. B.; Ortiz, J. V.; Cioslowski, J.; Fox, D. J. Gaussian 09, revision D.01; Gaussian, Inc.: Wallingford, CT, 2009.

76. 73. Anwar, J.; Tarling, S. E.; Barnes, P., Polymorphism of sulfathiazole. *J. Pharm. Sci.* **1989,** *78*, 337-342.

77. 74. Blagden, N.; Davey, R.; Lieberman, H.; Williams, L.; Payne, R.; Roberts, R.; Rowe, R.; Docherty, R., Crystal chemistry and solvent effects in polymorphic systems sulfathiazole. *J. Chem. Soc., Faraday Trans.* **1998,** *94*, 1035-1044.

78. 75. Caputo, G.; Reverchon, E., Use of urea as habit modifier in the supercritical antisolvent micronization of sulfathiazole. *Ind. Eng. Chem. Res.* **2007,** *46*, 4265-4272.

79. 76. Kordikowski, A.; Shekunov, T.; York, P., Polymorph control of sulfathiazole in supercritical CO_2. *Pharm. Res.* **2001,** *18*, 682-688.

80. 77. Yeo, S.-D.; Lee, J.-C., Crystallization of sulfamethizole using the supercritical and liquid antisolvent processes. *J. Supercrit. Fluids* **2004,** *30*, 315-323.

81. 78. Zeitler, J. A.; Newnham, D. A.; Taday, P. F.; Threlfall, T. L.; Lancaster, R. W.; Berg, R. W.; Strachan, C. J.; Pepper, M.; Gordon, K. C.; Rades, T., Characterization of temperature-induced phase transitions in five polymorphic forms of sulfathiazole by terahertz pulsed spectroscopy and differential scanning calorimetry. *J. Pharm. Sci.* **2006,** *95*, 2486-2498.

82. 79. McArdle, P.; Hu, Y.; Lyons, A.; Dark, R., Predicting and understanding crystal morphology: the morphology of benzoic acid and the polymorphs of sulfathiazole. *CrystEngComm* **2010,** *12*, 3119-3125.

83. 80. Parmar, M. M.; Khan, O.; Seton, L.; Ford, J. L., Polymorph selection with morphology control using solvents. *Cryst. Growth Des.* **2007,** *7*, 1635-1642.

84. 81. Bianco, S.; Caron, V.; Tajber, L.; Corrigan, O. I.; Nolan, L.; Hu, Y.; Healy, A. M., Modification of the solid-state nature of sulfathiazole and sulfathiazole sodium by spray drying. *AAPS PharmSciTech* **2012,** *13*, 647-60.

85. 82. Munroe, A.; Croker, D.; Rasmuson, Å. C.; Hodnett, B. K., Analysis of FII crystals of sulfathiazole: epitaxial growth of FII on FIV. *CrystEngComm* **2011,** *13*, 831-834.

86. 83. Hu, Y.; Erxleben, A.; Hodnett, B. K.; Li, B.; McArdle, P.; Rasmuson, Å. C.; Ryder, A. G., Solid-State Transformations of Sulfathiazole Polymorphs: The Effects of Milling and Humidity. *Cryst. Growth Des.* **2013,** *13*, 3404-3413.

87. Agarwal, V.; Peters, B., Solute precipitate nucleation: A review of theory and simulation advances. *Advances in Chemical Physics* **2014**, *155,* 97-160.

Scheme 1

Schematic definition of Non-Photochemical Laser-Induced Nucleation (NPLIN) experiments

Scheme 2

Molecular structure of sulfathiazole (STZ)

Table captions

Table 1.

Characteristics of the experiments reported in the different figures or tables. The ratio in column 4 to 7 represents the number of solutions where the nucleation has been observed versus the number of total irradiated solutions. Laser intensity, irradiation time and solution volume are also indicated.

Table 2.

Polymorph distributions of STZ crystals obtained by spontaneous nucleation in different solvents, from their supersaturated solutions of 130 % at 25 °C after 120 hours of slow evaporation. Characterization by Raman spectroscopy. 3 tubes *per* solvent were prepared. All the crystals obtained were gathered together. 15 crystals were randomly picked and analyzed.

Figure captions

Figure 1. Schematic representation of the experimental setup. (1) Laser, (2) wattmeter, (3) condenser, (4) mirror, (5) camera, (6) inverted microscope, (7) observation area, (8) exposure area and (9) cryothermostat. The red arrow indicates the inwards flow and the blue arrow the outwards flow. The whole setup is mounted on a trolley (grey). Reproduced from Clair *et al.*[6]

Figure 2. Solubility curve and metastable zone limit (MZL) of STZ (FIV) in water/ethanol ($^{v}/_{v}$ 1:1) tested for 168 hours.

Figure 3. *In situ* monitoring of nucleation process before and after laser irradiation, t_0 is the time (first pulse) of laser irradiation, the second photo is captured just after the irradiation (t = 6 s), the other photos are shot every 45 seconds. STZ in water/ethanol ($^{v}/_{v}$ 1:1), supersaturation coefficient 130%, laser intensity 0.23 GW/cm^2, LP, irradiation duration 5 seconds, scale bar 125 µm.

Figure 4. STZ crystal micrographs obtained by: (a) spontaneous nucleation, (b) LP laser intensity 0.23 GW/cm^2, irradiation time 10 s, (c) CP laser intensity 0.3 GW/cm^2, irradiation time 30 s. Supersaturation coefficient 130 % in water/ethanol ($^{v}/_{v}$ 1:1). Scale bar 125 µm.

Figure 5. Crystal habit micrographs of three STZ polymorphs (FII, FIII, FIV) crystallized *via* NPLIN. Characterization of these crystals by single crystal X-Ray Diffraction.

Figure 6. (a) Dependancy of nucleation efficiency on the supersaturation coefficient β and on laser intensity in the case of circular polarization (CP). (b). Dependancy of nucleation

efficiency on the supersaturation coefficient β and on laser intensity in the case of linear polarization (LP). In both cases the error bars are indicated. Irradiation time 60 s.

Figure 7. Evolution of $Ind_{50}(\beta)$ of STZ in water/ethanol ($^{v}/_{v}$ 1:1) at 25 °C with CP and LP and CBZ[44] in acetonitrile and methanol at 20 °C with CP and LP; the arrows represent the intersection of the LP and CP lines for a given set of conditions. Due to experimental error bars (Figure 6) estimation of the width of the fit is 0.1 GW/cm^2, on either sides of the fitted curves.

Figure 8. Dependency of the crystal size of STZ on irradiation time (LP 0.23 GW/cm^2, 130 %): (a) Irradiation duration = 1 s, (b) Irradiation duration = 5 s, (c) Irradiation duration = 10 s and (d) Irradiation duration = 30 s. All photos were captured 10 min after irradiation.

Figure 9. (a) Average number of crystals as a function of irradiation time (LP: 0.23 GW/cm^2, CP 0.3 GW/cm^2). The insert is a zoom for 1s. (b) Average size as a function of the irradiation time (LP: 0.23 GW/cm^2, CP 0.3 GW/cm^2).

Figure 10. Polymorph distribution ratio obtained by spontaneous nucleation, NPLIN (LP) and NPLIN (CP). The number of characterized crystals is given for each polymorph. The number of tubes used is given in Table 1. Irradiation time 60 s.

Figure 11. Schematic representation of the interaction energy for carbamazepine adapted from ref 47.

Figure 12. Interaction energy ($kJ.mol^{-1}$) for STZ polymorphic form II, III and IV *versus* the rank of the interaction energy (1 is the strongest interaction for each polymorph). The packing corresponding to the different range of interaction energy is given for each polymorph in decreasing order of stability. Symmetry of these packing is indicated in black.

Table 1

	Nucleation type	110 (%)	120 (%)	130 (%)	170 (%)	Laser intensity ($GW.cm^{-2}$)	Irradiation time (s)	Solution volume (ml)
Table 2	spontaneous			*				
Figure 3	NPLIN			1**			60	1
Figure 6a	NPLIN (CP)	4/20	4/14	8/18	8/10	0.15	60	1
	NPLIN (CP)	3/12	5/15	11/13	9/10	0.22	60	1
	NPLIN (CP)	9/25	7/15	19/29	10/10	0.30	60	1
Figure 6b	NPLIN (LP)	3/13	5/13	10/18		0.13	60	1
	NPLIN (LP)	5/14	6/11	18/26		0.19	60	1
	NPLIN (LP)	8/14	9/13	12/13		0.23	60	1
Figure 9	NPLIN (LP)	4/4		4/4		0.23	1, 5, 10, 20, 30	1
	NPLIN (CP)			3/3		0.30	1, 5, 10, 20, 30	1
Figure 10	spontaneous			3/3				
	NPLIN (LP)			35/35		0.23	60	1
	NPLIN (CP)			27/27		0.30	60	1

* 3 tubes, 15 crystals

** $t_{NPLIN} \in [0.026; 0.5]$ h has been determined over 336 tubes

Table 2

Method	Solvents	I	II	III	IV	V	Total
Spontaneous nucleation	water/ethanol ($^{v}/_{v}$ 1:1)	0	1	7	7	0	15
	n-propanol	9	1	2	2	1	15
	ethanol	0	6	5	4	0	15
	water	0	0	3	10	2	15

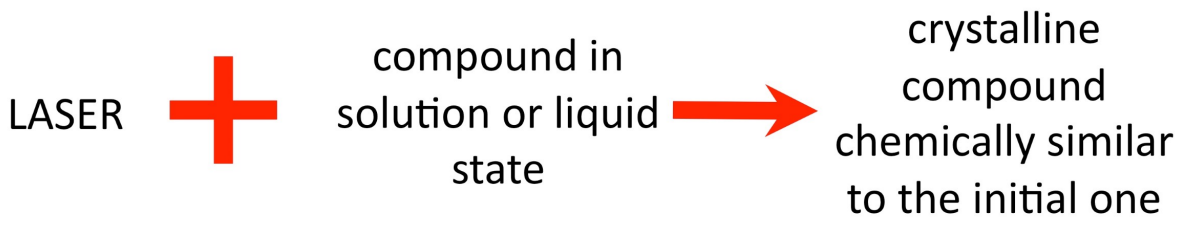
LASER
compound in solution or liquid state
crystalline compound chemically similar to the initial one

Scheme 1

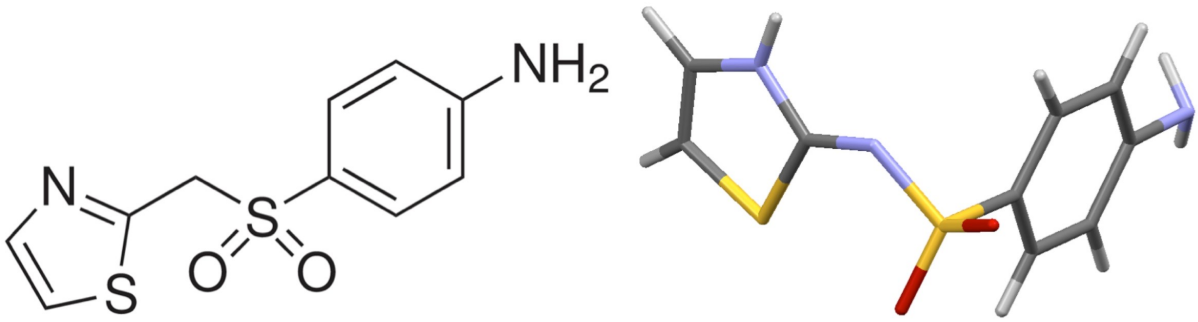

Scheme 2

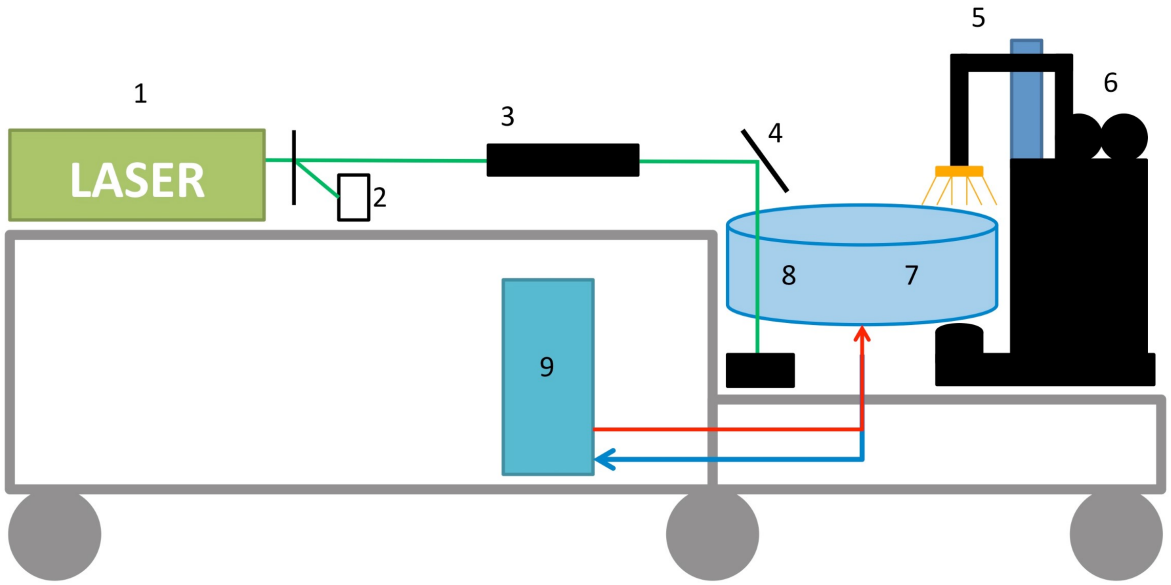

Figure 1

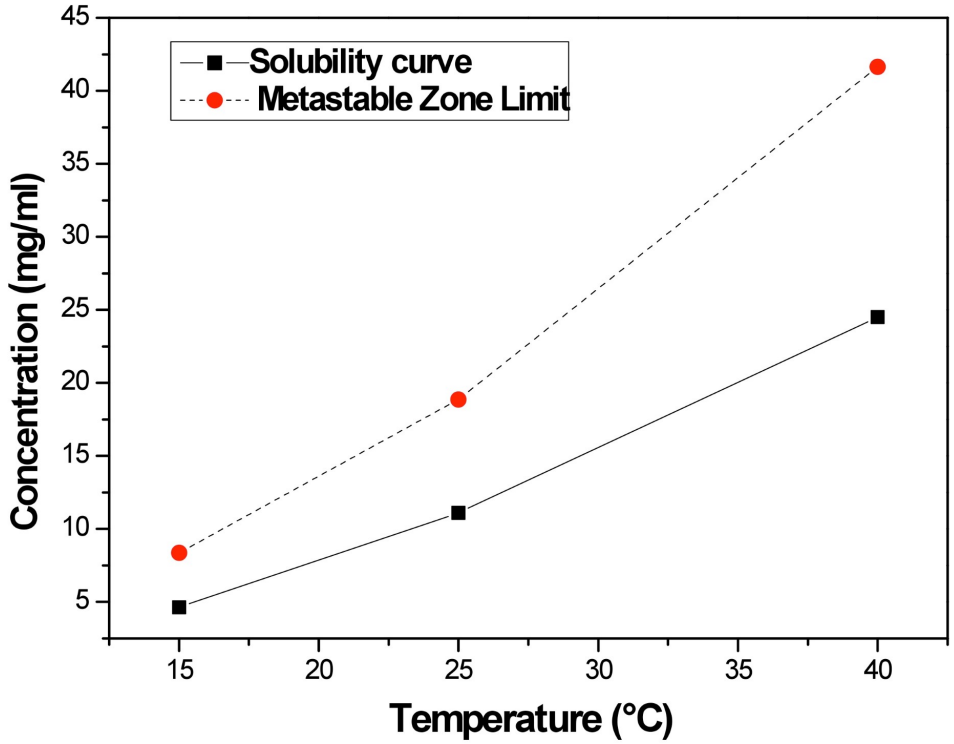
Solubility curve
Metastable Zone Limit
Concentration (mg/ml)
Temperature (°C)
45
40
35
30
25
20
15
10
5
15
20
25
30
35
40

Figure 2

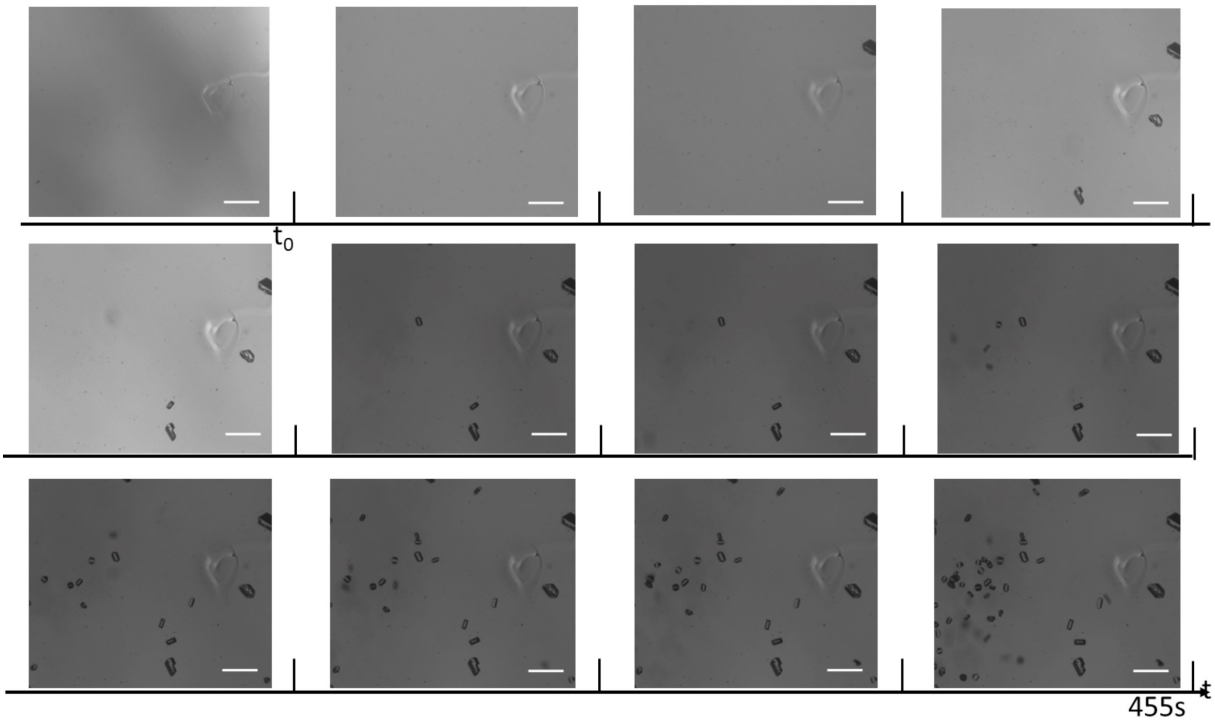

Figure 3

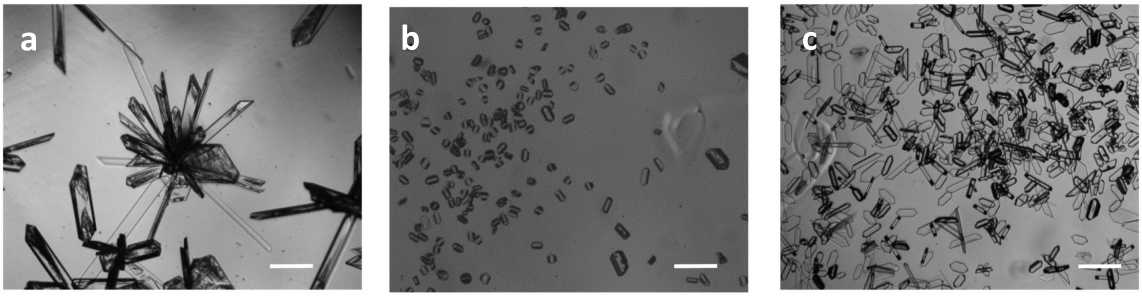

Figure 4

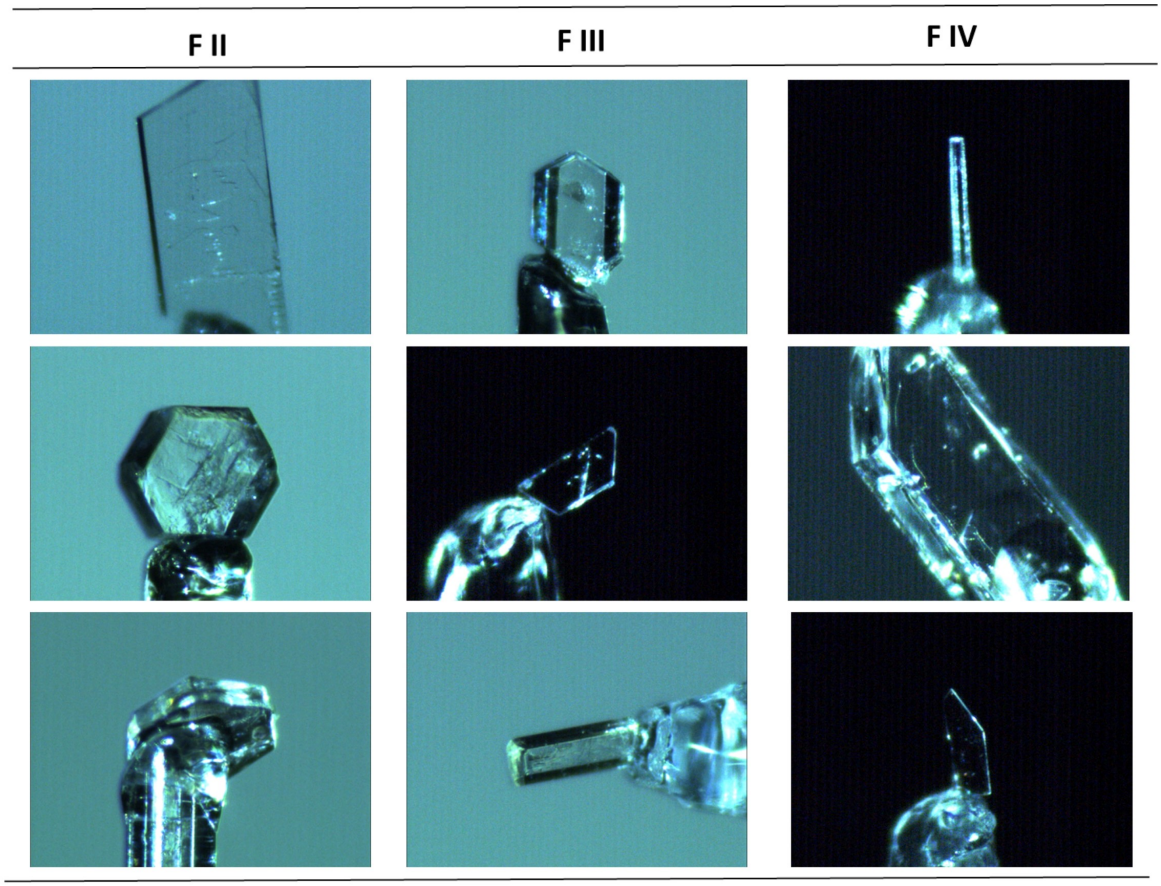

Figure 5

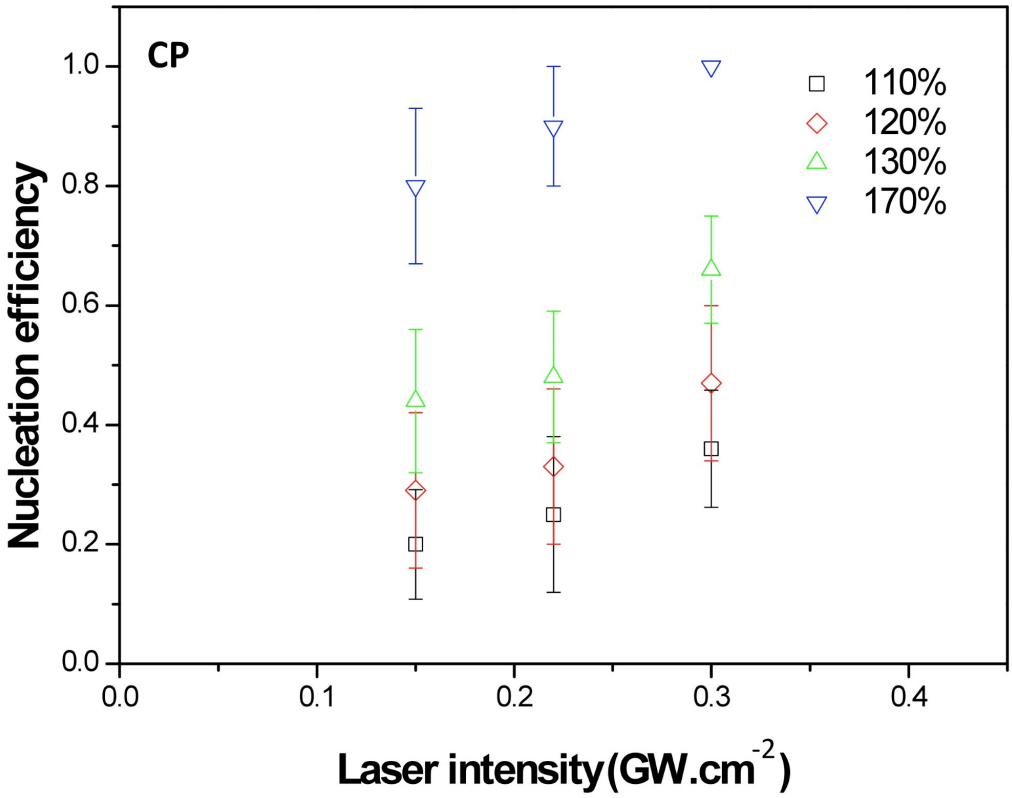
CP
110%
120%
130%
170%
Nucleation efficiency
Laser intensity(GW.cm-2)
0.0
0.2
0.4
0.6
0.8
1.0
0.0
0.1
0.2
0.3
0.4

Figure 6 a

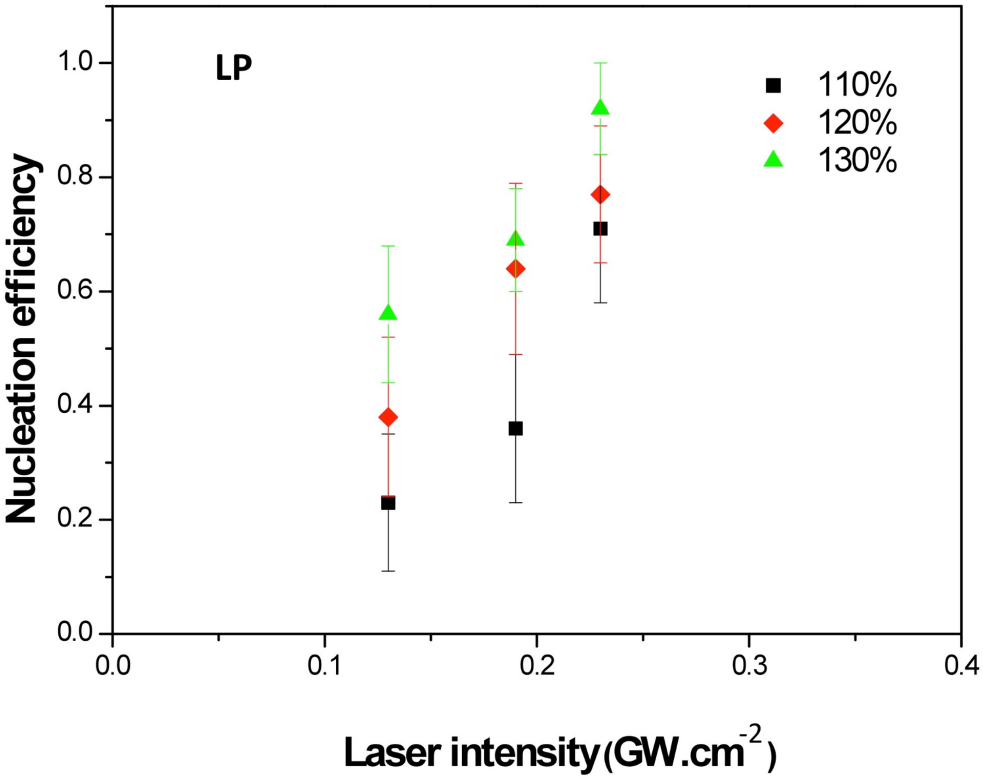
LP
110%
120%
130%
Nucleation efficiency
1.0
0.8
0.6
0.4
0.2
0.0
0.0
0.1
0.2
0.3
0.4
Laser intensity(GW.cm-2)

Figure 6 b

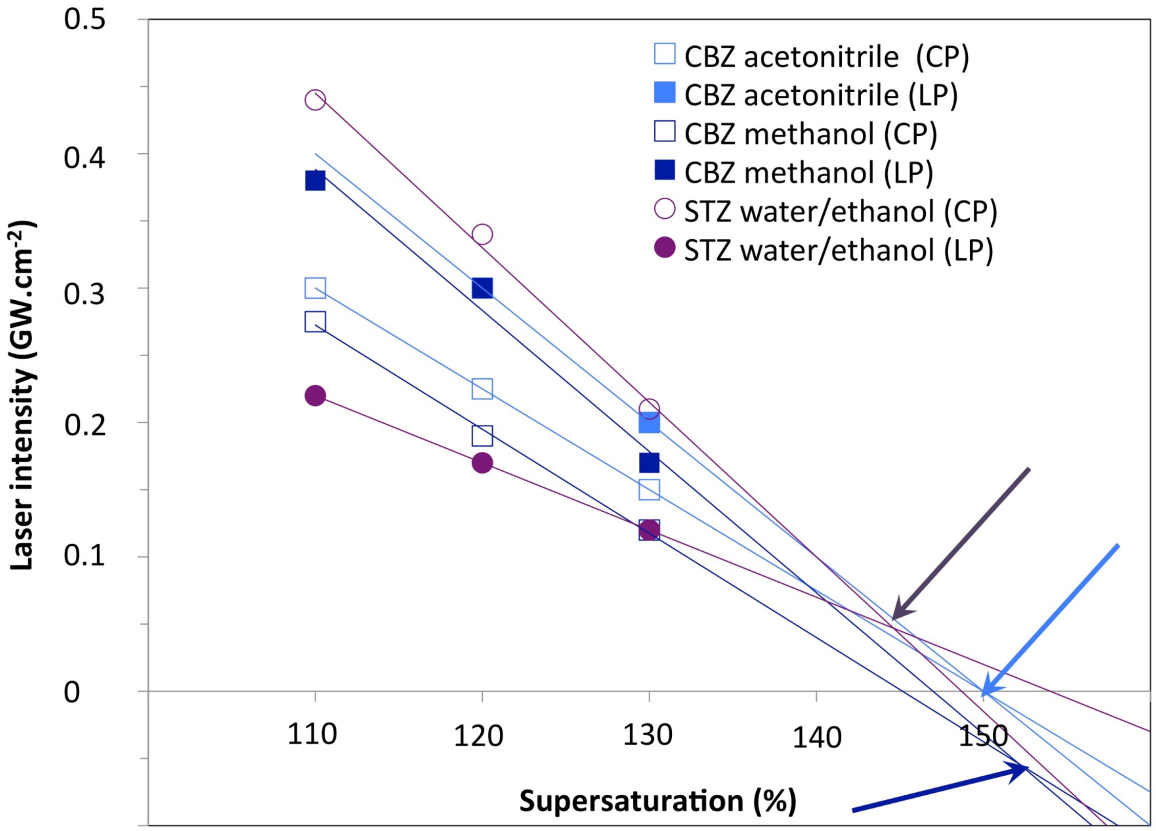
0.5
0.4
0.3
0.2
0.1
0
Laser intensity (GW.cm-2)
110
120
130
140
150
Supersaturation (%)
CBZ acetonitrile (CP)
CBZ acetonitrile (LP)
CBZ methanol (CP)
CBZ methanol (LP)
STZ water/ethanol (CP)
STZ water/ethanol (LP)

Figure 7

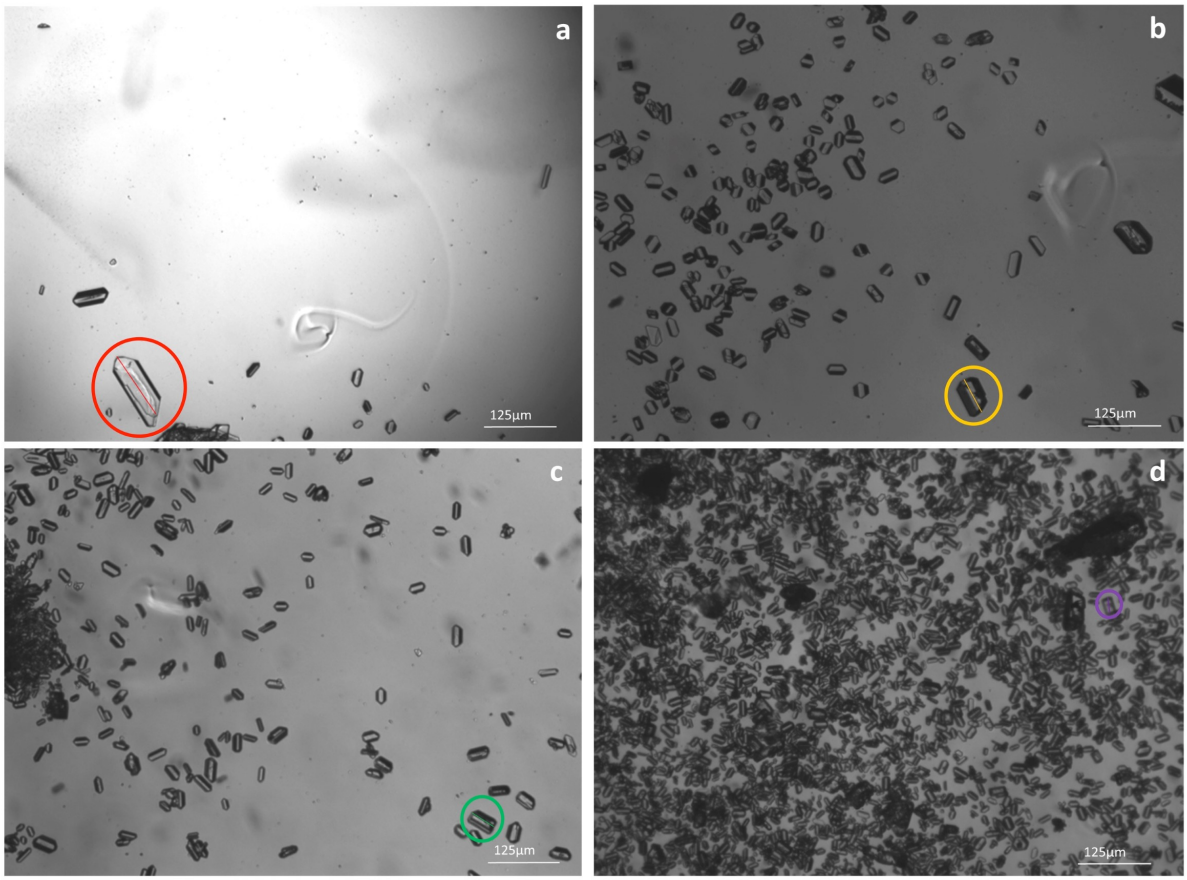

Figure 8

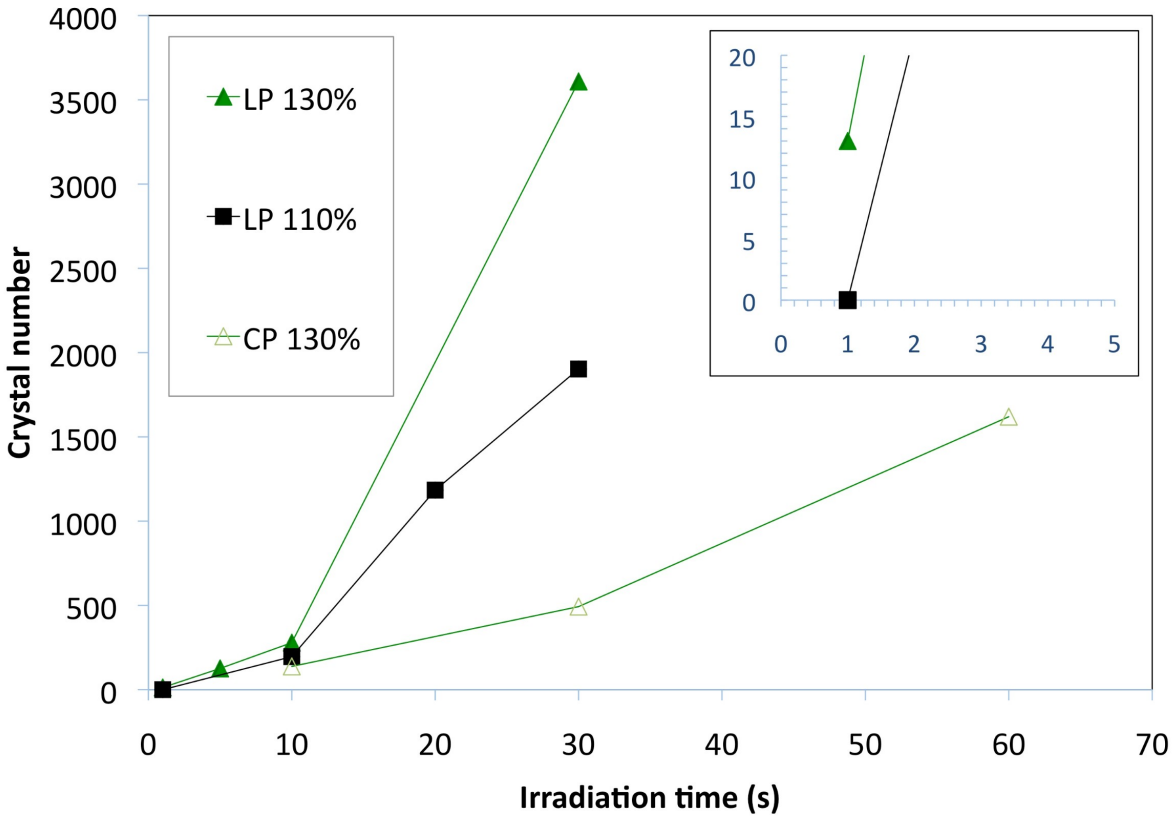
4000
3500
3000
2500
2000
1500
1000
500
0
Crystal number
0
10
20
30
40
50
60
70
Irradiation time (s)
LP 130%
LP 110%
CP 130%
20
15
10
5
0
0
1
2
3
4
5

Figure 9a

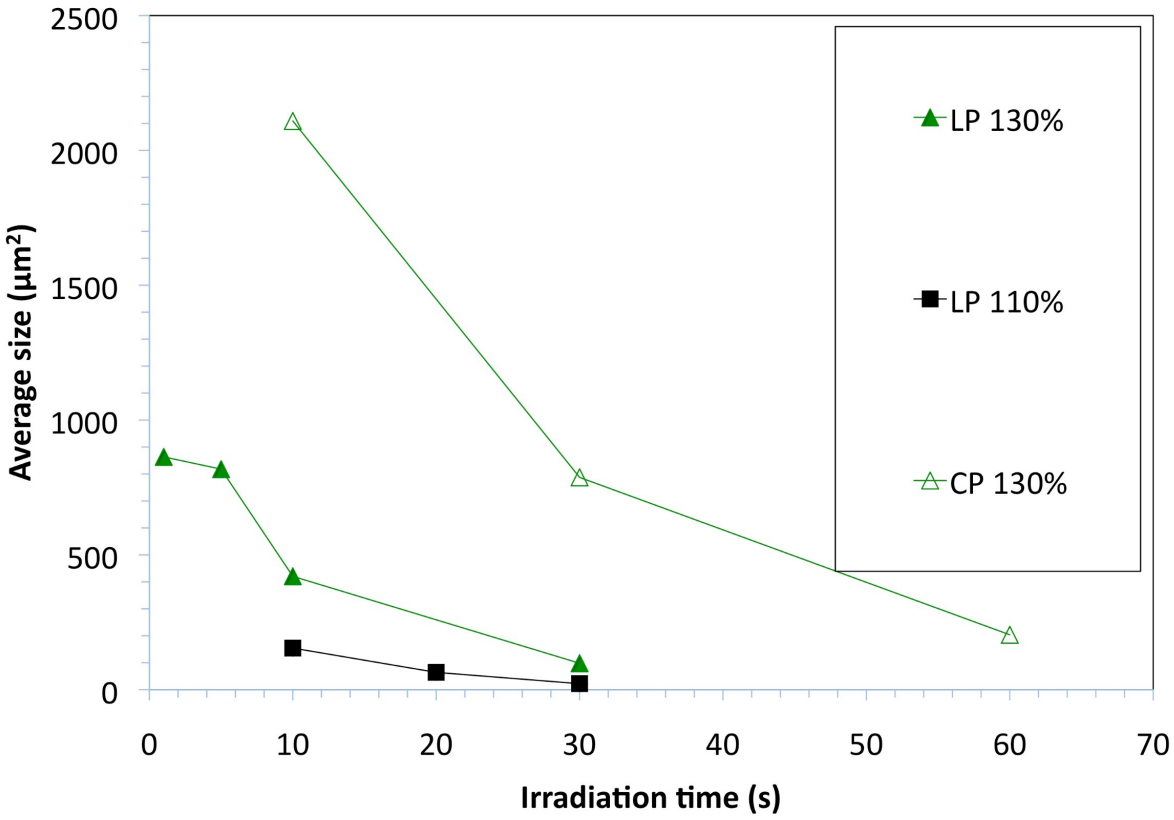
2500
2000
1500
1000
500
0
Average size (µm²)
0
10
20
30
40
50
60
70
Irradiation time (s)
LP 130%
LP 110%
CP 130%

Figure 9b

.

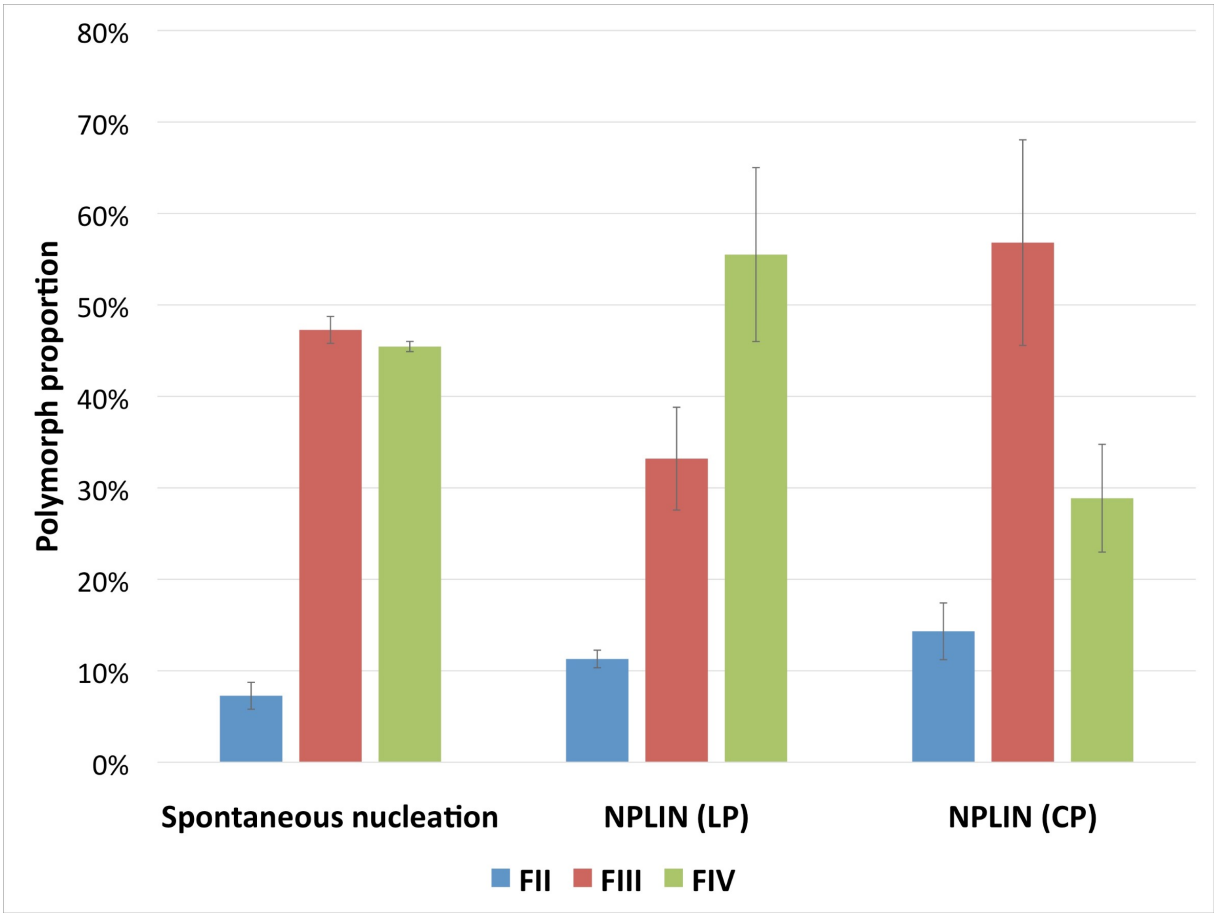
80%
70%
60%
50%
40%
30%
20%
10%
0%
Polymorph proportion
Spontaneous nucleation
NPLIN (LP)
NPLIN (CP)
FII
FIII
FIV

Figure 10

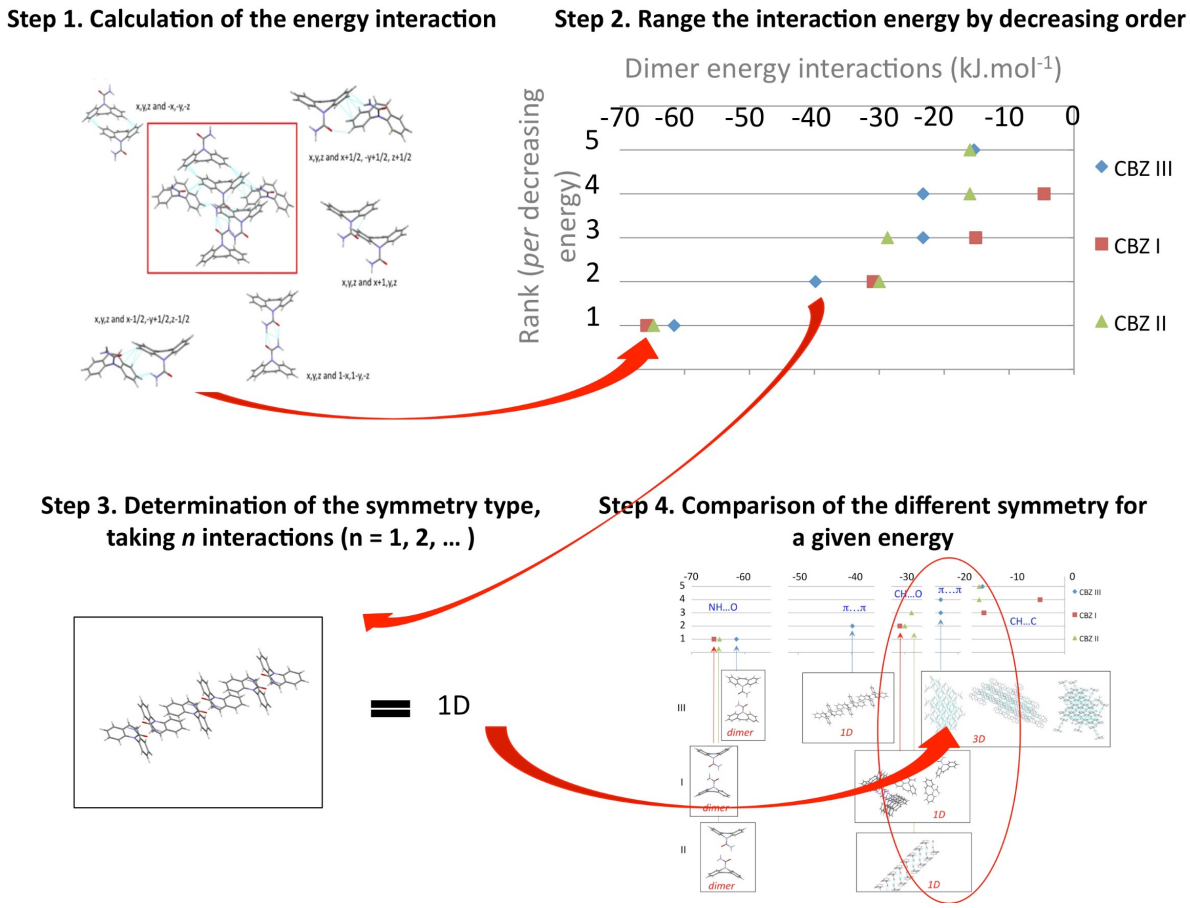
Step 1. Calculation of the energy interaction
Step 2. Range the interaction energy by decreasing order
Dimer energy interactions (kJ.mol-1)
Rank (per decreasing energy)
-70 -60 -50 -40 -30 -20 -10 0
5
4
3
2
1
CBZ III
CBZ I
CBZ II
Step 3. Determination of the symmetry type, taking n interactions (n = 1, 2, …)
1D
Step 4. Comparison of the different symmetry for a given energy
NH...O
π....π
CH...O
CH...C
dimer
1D
3D

Figure 11

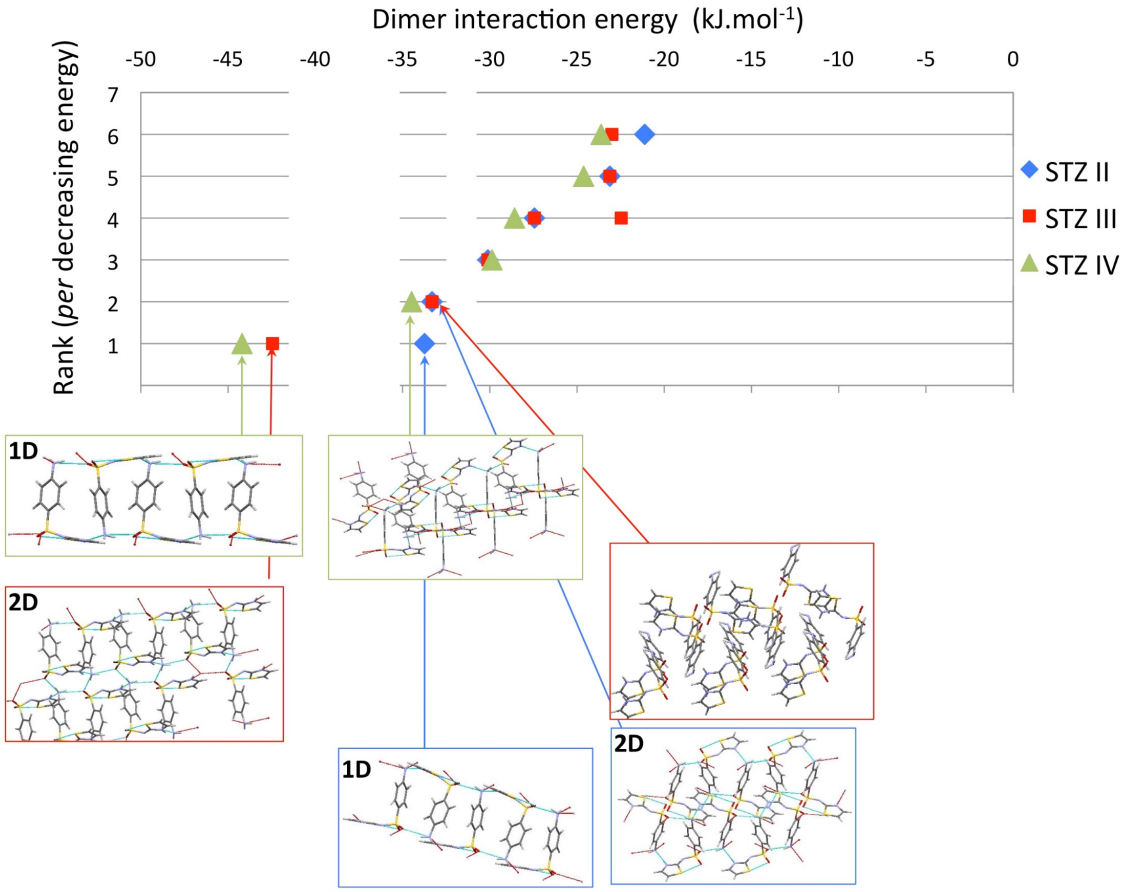
Dimer interaction energy (kJ.mol-1)
-50
-45
-40
-35
-30
-25
-20
-15
-10
-5
0
Rank (per decreasing energy)
7
6
5
4
3
2
1
STZ II
STZ III
STZ IV
1D
2D
1D
2D

Figure 12

For Table of Contents Use Only

Non-Photochemical Laser-Induced Nucleation of sulfathiazole in water/ethanol mixture

LI Wenjing, IKNI Aziza, SCOUFLAIRE Philippe, SHI Xiaoxuan, EL HASSAN Nouha, GILLET Jean-Michel, SPASOJEVIĆ-DE BIRÉ Anne

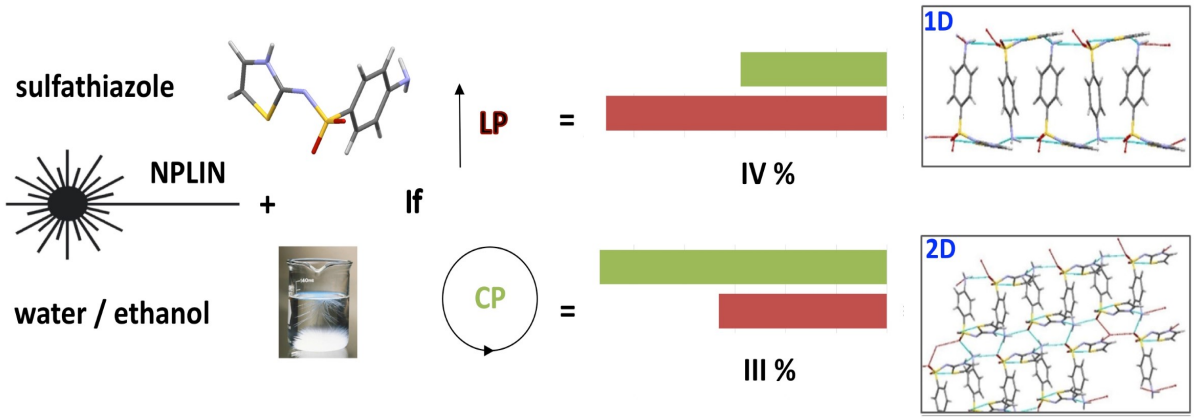

Nucleation induction time and crystal habits of sulfathiazole (STZ) crystallized by Non-Photochemical Laser-Induced Nucleation (NPLIN) have been compared with those obtained by spontaneous nucleation. A dependency of STZ crystal size and crystal number on the irradiation duration, i.e., pulse number, has been established. The role of the laser polarization (linear or circular) has been demonstrated in comparison with spontaneous nucleation. In order to gain a deeper understanding of this behavior, we have calculated the *ab initio* interaction energies for all dimers existing in the different STZ polymorphs. The theoretical results are coherent with observation.